Journal of Medicinal Chemistry

Article

pubs.acs.org/jmc

Design, Synthesis, and Biological Evaluation of Novel Conformationally Constrained Inhibitors Targeting Epidermal Growth Factor Receptor Threonine^{790} → Methionine^{790} Mutant

Shaohua Chang,[†,§,#] Lianwen Zhang,[§,‡,#] Shilin Xu,[†,§] Jinfeng Luo,[†] Xiaoyun Lu,[†] Zhang Zhang,[†] Tianfeng Xu,[†,§] Yingxue Liu,[†] Zhengchao Tu,[†] Yong Xu,[†] Xiaomei Ren,[†] Meiyu Geng,[⊥] Jian Ding,[⊥] Duanqing Pei,[†] and Ke Ding*[,†]

[†]Key Laboratory of Regenerative Biology and Institute of Chemical Biology, Guangzhou Institutes of Biomedicine and Health, Chinese Academy of Sciences, #190 Kaiyuan Avenue, Guangzhou 510530, China

[‡]School of Life Science, University of Science and Technology of China, # 96 Jinzhai Road, Hefei 230026, China

[§]Graduate School of Chinese Academy of Sciences, # 19 Yuquan Road, Beijing 100049, China

[⊥]State Key Laboratory of Drug Research, Shanghai Institute of Materia Medica, Chinese Academy of Sciences, # 555 Zu-Chong-Zhi Road, Zhangjiang Hi-Tech Park, Shanghai 201203, China

Supporting Information

ABSTRACT: The EGFR^{T790M} mutant contributes approximately 50% to clinically acquired resistance against gefitinib or erlotinib. However, almost all the single agent clinical trials of the second generation irreversible EGFR inhibitors appear inadequate to overcome the EGFR^{T790M}-related resistance. We have designed and synthesized a series of 2-oxo-3,4-dihydropyrimido[4,5-*d*]pyrimidinyl derivatives as novel EGFR inhibitors. The most potent compounds, **2q** and **2s**, inhibited the enzymatic activities of wild-type and mutated EGFRs, with IC_{50} values in subnanomolar ranges, including the T790M mutants. The kinase inhibitory efficiencies of the compounds were further validated by Western blot analysis of the activation of EGFR and downstream signaling in cancer cells harboring different mutants of EGFR. The compounds also strongly inhibited the proliferation of H1975 non small cell lung cancer cells bearing EGFR$^{L858R/T790M}$, while being significantly less toxic to normal cells. Moreover, **2s** displayed promising anticancer efficacy in a human NSCLC (H1975) xenograft nude mouse model.

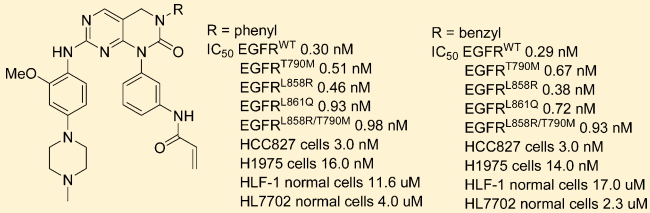

INTRODUCTION

Epidermal growth factor receptor (EGFR) belongs to the ErbB family of receptor tyrosine kinases which play indispensable roles in cell proliferation, survival, adhesion, migration, and differentiation.[1] Small molecular EGFR inhibitors, gefinitib and erlotinib, were approved by US Food and Drug Administration in 2002 and 2004, respectively, and have achieved significant clinical benefit for non small cell lung cancer (NSCLC) patients harboring activating EGFR mutations such as L858R or exon 19 deletions (del E746-A750), etc.[2−4] Anti-EGFR antibodies cetuximab[5] and panitumumab[6] have also become effective clinical therapies for different solid tumors associated with overexpressed EGFR. Despite the clear clinical benefits of gefinitib and erotinib, their efficacy is eventually diminished because of acquired point mutations in the kinase domain of EGFR as well as the upregulation of bypass signaling pathways.[7] Particularly, a single T790M point mutation (threonine^{790} → methionine^{790}) at the "gatekeeper" position in EGFR accounts for approximately 50% in clinically acquired resistant patients.[8] Different from the fact that T315I-mutated Abl introduces a steric impediment for imatinib binding,[9] EGFR^{T790M} only moderately affects the binding of gefinitib and erotinib. However, this mutation enhances the binding affinity for ATP with EGFR, which leads to higher concentrations of the competitive inhibitors being required for the kinase suppression.[10]

In order to overcome the T790M mutation related resistance, a number of irreversible ATP-competitive EGFR inhibitors[11] such as CI-1033,[12] BIBW2992,[13] HKI-272,[14] and PF00299804,[15] etc., have been developed. The irreversible inhibitors contain a Michael addition receptor moiety which may form a covalent bind with the conserved cysteine residue present in the lip of the EGFR ATP binding site (Cys797) to achieve occupancy greater than that of the reversible inhibitors.[16] The reaction of the Cys797 residue with irreversible inhibitors also potently prevents its sulfenylation-enhancing kinase activity.[30] However, almost all the single agent clinical trials of the second generation irreversible EGFR inhibitors seemed to be disappointing.[7b] For instance, HKI-272

Received: November 25, 2011
Published: February 16, 2012

(neratinib) has been demonstrated to show little activity against gefitinib-resistant NSCLC patients harboring EGFR mutations in a phase II trial, likely due to toxicity-related dose-limitation.[17] PF00299804 also failed to show any responses in NSCLC patients with $EGFR^{T790M}$ mutants.[18] In a phase III clinical trial, BIBW2992 (afatinib) only displayed 7% response rate for NSCLC patients who progressed after ≥12 weeks of gefinitib or erlotinib treatment.[7b,19] The most promising results came from a phase Ib trial of a combination of BIBW2992 with cetuximab, which showed an approximate 40% objective response rate. However, the progression-free survival and overall survival results are unpredictable.[20] Therefore, the clinically acquired resistance against first-line EGFR inhibitors remains one of the major challenging unmet medical needs for NSCLC treatment. It is highly desirable to identify new molecules targeting $EGFR^{T790M}$ mutants.[11]

Most recently, Gray et al. reported a novel series of substituted pyrimidines as irreversible EGFR inhibitors displaying good selectivity against $EGFR^{T790M}$ mutants over the wild type kinase.[21] One of the most active and selective inhibitors, WZ4002 (**1**),[21] potently inhibited the proliferation of the cancer cells or Ba/F3 cells harboring L858R, del E746-A750, and/or T790M mutated EGFR, while it was obviously less potent against the growth of wild type EGFR cells. Furthermore, the compound also displayed promising in vivo efficacy in gefitinib-resistant NSCLC models, which represented a new, promising strategy to overcome the acquired resistance for NSCLC patients. The clinical results of **1** or related candidates are eagerly awaited. In this paper, we report the structural design, synthesis, and biological evaluation of conformation-constrained 2-oxo-3,4-dihydropyrimido[4,5-*d*]-pyrimidinyl derivatives as novel EGFR inhibitors which strongly suppressed the enzymatic activities of $EGFR^{WT}$, $EGFR^{L858R}$, $EGFR^{T790M}$, $EGFR^{L861Q}$, and $EGFR^{L858R/T790M}$. The compounds also potently inhibited the proliferation of NSCLC cells bearing $EGFR^{del\ E746\text{-}A750}$ or $EGFR^{L858R/T790M}$ mutants. One of the most potent inhibitors, **2s**, displayed significant in vivo anticancer efficacy in a H1975 human NSCLC cancer xenograft mouse model, representing a new, promising lead compound with a different chemical scaffold for further development of EGFR inhibitors to overcome $EGFR^{T790M}$ mutation-induced clinical resistance to gefitinib and erotinib.

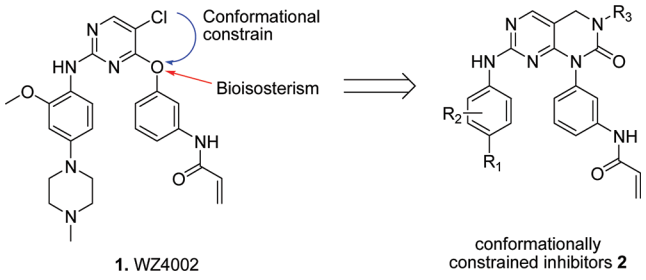

Figure 1. Design of conformation-constrained derivatives of **1** as new EGFR inhibitors.

CHEMISTRY

The designed compounds **2** were prepared by using ethyl 4-chloro-2-(methylthio)pyrimidine-5-carboxylate (**3**) as the starting material (Scheme 1).[29] Briefly, a direct nucleophilic coupling of compound **3** with *tert*-butyl 3-aminophenylcarbamate (**4**) almost quantitatively produced ethyl 4-(3-(*tert*-butoxycarbonyl)phenylamino)-2-(methylthio)pyrimidine-5-carboxylate (**5**) as a white solid. The reduction of compound **5** with lithium aluminum hydride yielded *tert*-butyl 3-(5-(hydroxymethyl)-2-(methylthio)pyrimidin-4-ylamino)-phenylcarbamate (**6**) which was followed by selective oxidation to produce the aldehyde **7** in a good yield. A variety of diamine intermediates **8** could be prepared by a reductive amination of aldehyde **7** with different amines. With diamine compounds **8** in hand, the key intermediates **10** were readily synthesized by direct cyclization with triphosgene and followed by oxidation. Compound **10** coupled with different substituted anilines to produce precursor compounds **11** which were further deprotected with trifluoroacetic acid and reacted with acryloyl chloride to obtain the conformation-constrained EGFR inhibitors **2**.

RESULTS AND DICUSSION

Taking **1** as the lead molecule, we designed a series of 2-oxo-3,4-dihydropyrimido[4,5-*d*]pyrimidinyl derivatives as new EGFR inhibitors using a combination of bioisosterism and conformational constraint strategies. The kinase inhibitory activities of the designed compounds were evaluated via a well established FRET-based Z′-Lyte assay[22] against different types of EGFR kinases, and the results are summarized in Table 1. Under the experimental conditions, compound **1** potently inhibited $EGFR^{WT}$, $EGFR^{T790M}$, $EGFR^{L858R}$, $EGFR^{L861Q}$, and $EGFR^{L858R/T790M}$ with IC_{50} values of 6.18, 3.77, 5.37, 6.13, and 1.88 nM, respectively, which were similar to previously reported data.[21]

We were pleased to find that the conformation-constrained compound **2a** also strongly suppressed the enzymatic activities of all five types of EGFR kinases with potencies comparable to that of compound **1** (Table 1). Taking compound **2a** as our new lead compound, we conducted further structure modification to explore the structure−activity relationships. The impact of the 1-(4-methylpiperazinyl) group in compound **2a** was first inspected by removal or replacement with other moieties. The results demonstrated that the 1-(4-methylpiperazinyl) group was important for the EGFR kinase inhibition. When the 1-(4-methylpiperazinyl) group was removed (**2g**) or replaced with dimethylamino (**2b**), 1-piperidinyl (**2c**), or *N*-morpholino (**2d**) moieties, the potencies against EGFR kinases decreased approximately 5−20 fold. For instance, the IC_{50} values of compound **2a** against $EGFR^{WT}$, $EGFR^{T790M}$, $EGFR^{L858R}$, $EGFR^{L861Q}$, and $EGFR^{L858R/T790M}$ were 1.16, 6.56, 1.08, 1.21, and 3.14 nM, while the corresponding values for compound **2c** were decreased to 29.50, 95.71, 10.42, 15.40, and 36.43 nM, respectively. Further investigation also revealed that the potency loss of compound **2c** was partially restored by introducing a 4-dimethylamino group (**2b**) at the position of the original piperidinyl moiety. When the 1-(4-methylpiperazinyl) group was replaced with a 1-(4-methyl-1,4-diazepanyl) group, the resulting compound **2e** was almost equally potent to compound **2a**. However, when the substituted aniline in compound **2a** was replaced with a simple methylamino moiety (**2h**), the potencies against EGFR kinases were almost completely abolished.

The impact of the R_2 methoxy group in **2a** was also investigated. Similar to the previous observation,[21] removal of the R_2 methoxy group improved the potencies against all forms of the EGFR kinases 2- to 3-fold, but the resulting compound **2i** could lose the selectivity over JAK3 and the TEC-family

dx.doi.org/10.1021/jm201591k | J. Med. Chem. 2012, 55, 2711−2723

Scheme 1. Synthesis of the Conformation-Constrained Compounds 2

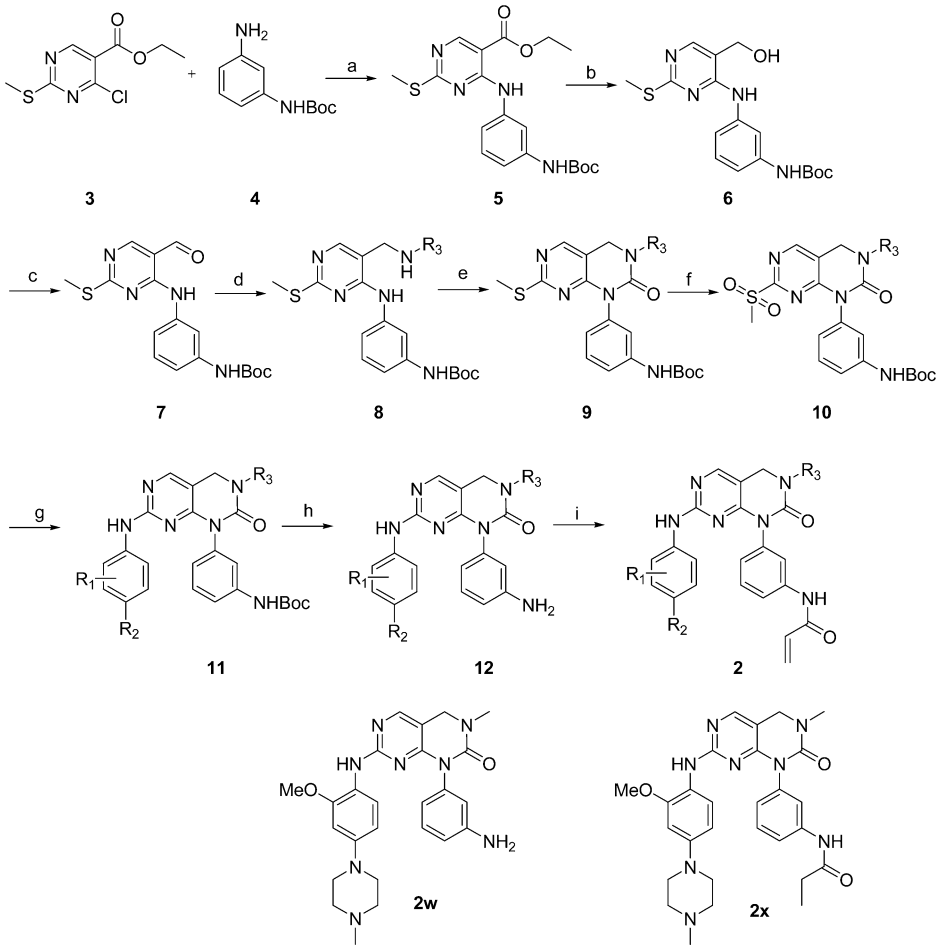

Reagent and conditions: (a) K_2CO_3 (2.0 equiv), dimethylformamide (DMF), 60 °C, overnight, 97%; (b) lithium aluminum hydride (LAH, 2.0 equiv), THF, −40 °C to r.t., 57%; (c) MnO_2, dichloromethane, r.t., overnight, 85%; (d) R^2NH_2, AcOH, $NaBH_4$, MeOH, 0 °C to r.t., overnight; (e) triphosgene (0.34 equiv), Et_3N (4.0 equiv), 0 °C to r.t., 2.0 h; (f) 3-chloroperbenzoic acid (*m*-CPBA, 3.0 equiv), dichloromethane, r.t., 3.0 h; (g) R^1NH_2 (1.0 equiv), trifluoroacetic acid (1.0 equiv), 2-BuOH, 110 °C, sealed tube, 18.0 h, 30−60%; (h) trifluoroacetic acide, dichloromethane, r.t.; (i) acryloyl chloride (1.0 equiv), *N*,*N*-diisopropylethylamine (DIPEA, 1.0 equiv), 0 °C to r.t.

kinase.[21] When the methoxy group was moved from the 2′-position to the 3′-position (**2j**), the inhibitory potency against $EGFR^{L858R/T790M}$ was barely affected, although the potencies against $EGFR^{WT}$, $EGFR^{T790M}$, and $EGFR^{L858R}$ were improved 2−3 fold. When the 2′-methoxy group in **2a** was replaced with a slightly larger group such as an ethoxy (**2k**) or isopropoxy (**2l**) group, potencies were obviously decreased. Although the 2′-methyl analogue (**2m**) displayed potencies similar to that of **2a**, the 2′-fluoro compound (**2n**) was totally inactive. The potency loss of **2n** might be due to a five-membered ring formation involving a hydrogen bond between the F atom and the NH moiety, which could alter the conformation of the molecule.

The results also illustrated that the R_3 position in compound **2a** might be replaced with a larger hydrophobic group to improve the potency against EGFR kinase. When the R_3 methyl was replaced with an isopropyl (**2o**) or cyclopropyl (**2p**) group, the inhibitory activities against $EGFR^{WT}$, $EGFR^{L858R}$, and $EGFR^{L861Q}$ were obviously improved, with IC_{50} values below 1 nM, but the suppressive functions against $EGFR^{T790M}$ and $EGFR^{L858R/T790M}$ were slightly decreased. The methyl group could also be replaced with large hydrophobic groups such as 2-naphthyl (**2r**), 4-biphenyl (**2t**), 4-phenoxyphenyl (**2u**), and 4-benzoxyphenyl (**2v**), etc., to maintain the strong inhibition against EGFR kinase. Interestingly, when the R_3 methyl in compound **2a** was replaced with a phenyl (**2q**) or benzyl (**2s**) group, the resulting compounds showed the best potencies. For instance, compound **2s** strongly bound to all the types of EGFR kinase and inhibited their enzymatic functions with K_d and IC_{50} values both in subnanomolar ranges (Table 1), which is obviously more potent than compound **1**. However, the binding affinities with EGFR were significantly decreased over 1000 fold (K_d values about 560−1500 nM) when the α,β-unsaturated acrylamide moieties were removed (**2w** and **2x**). Highly consistent with their binding affinity loss, **2w** and **2x** were almost totally inactive to inhibit the EGFR enzymatic activities (IC_{50} values >1000 nM).

Taking compounds **2q** and **2s** as examples, we further profiled the compounds against a panel of 451 kinases using the Ambit Kinome screening platform to investigate the selectivity of the new EGFR inhibitors (Supporting Information and Figure 2). The results suggested that both compounds displayed excellent selectivity on EGFR, and the specificity profile of compound **2s** was obviously greater than that of **2q**. In addition to EGFR, **2s** only exhibited obvious binding to BLK, BTK, ErbB-2, ErbB4, GAK, and TXK at a concentration of 100 nM, which was about 100 times its K_d values on EGFR,

dx.doi.org/10.1021/jm201591k | J. Med. Chem. 2012, 55, 2711−2723

Table 1. In Vitro Enzymatic Inhibitory Activities of Compounds 2 against Different Types of EGFR[a]

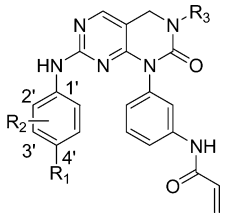

Compounds	R_1	R_2	R_3	EGFR IC_{50} (nM)				
				WT	T790M	L858R	L861Q	L858R/T790M
1				6.18 (46) [b, c]	3.77	5.37 (29) [b, c]	6.13	1.88
2a		2'-MeO	Me	1.16	6.56	1.08	1.21	3.14
2b		2'-MeO	Me	4.99	24.90	4.95	6.22	11.50
2c		2'-MeO	Me	29.50	95.71	10.42	15.40	36.43
2d		2'-MeO	Me	16.40	60.31	10.33	12.74	28.85
2e		2'-MeO	Me	1.47	11.0	2.11	2.75	5.17
2f		2'-MeO	Me	3.52	9.52	2.41	2.83	5.20
2g	H	H	Me	6.95	45.7	10.9	12.1	28.3
2h	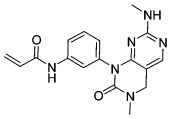			929	>1000	>1000	837.1	>1000
2i		H	Me	0.43	1.66	0.53	0.56	1.19
2j		3'-MeO	Me	0.41	1.67	0.63	2.31	2.04
2k		2'-EtO	Me	4.41	12.7	2.68	3.02	7.10
2l		2'-Pr(i)O	Me	8.81	39.9	13.7	13.5	36.3
2m		2'-Me	Me	1.95	9.37	1.21	1.31	4.18
2n		2'-F	Me	>1000	>1000	>1000	>1000	>1000
2o		2'-MeO	i-Pr	0.38	6.02	0.45	0.46	4.42
2p		2'-MeO	Cyclo-Pr	0.58	10.5	0.66	0.73	6.02
2q		2'-MeO	Ph	0.30	0.51	0.46	0.93	0.98
2r		2'-MeO	2-naphthyl	0.80	1.34	1.16	1.59	2.44
2s		2'-MeO	Bn	0.29 (1.2) [b]	0.67 (0.29) [b]	0.38 (1.3) [b]	0.72 (0.68) [b]	0.93 (0.30) [b]
2t		2'-MeO	4-biphenyl	1.41	5.24	1.67	3.43	4.64
2u		2'-MeO	4-phenoxyphenyl	1.52	2.03	1.66	2.31	3.57
2v		2'-MeO	4-benzoxyphenyl	1.67	2.43	2.42	2.56	6.31
2w				>1000	>1000	478	>1000	>1000
2x				>1000 (1400) [b]	>1000 (560) [b]	>1000 (1600) [b]	>1000 (1100) [b]	>1000 (850) [b]

[a]EGFR activity assays were performed using the FRET-based Z′-Lyte assay according to the manufacturer's instructions. The compounds were incubated with the kinase reaction mixture for 1.5 h before measurement. The data were means from at least three independent experiments.

dx.doi.org/10.1021/jm201591k | J. Med. Chem. 2012, 55, 2711−2723

Table 1. continued

*b*Binding constant values (K_d) were determined from Ambit KINOMEscan. The data were means from two independent experiments. *c*Reported data.[21]

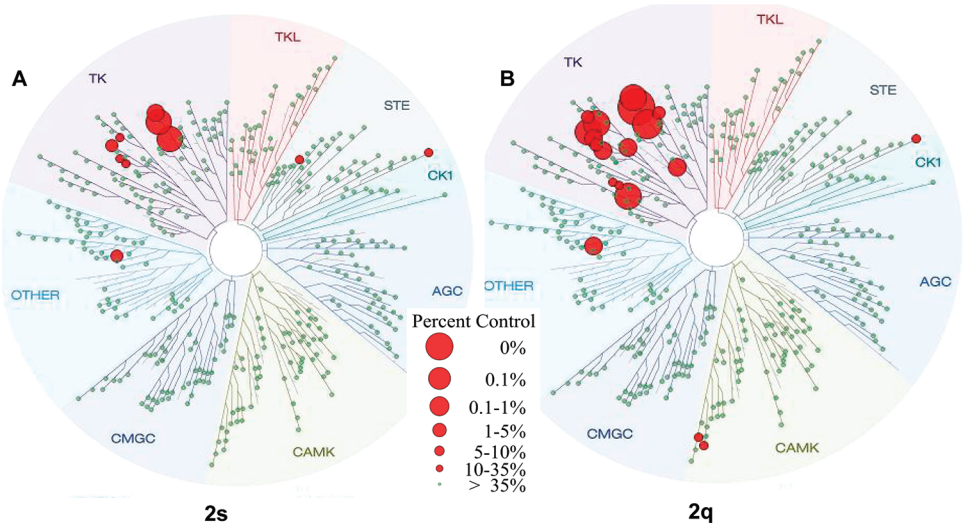

Figure 2. KINOMEsacn tree spot maps illustrating the selectivity profiles for compounds **2q** and **2s** versus a panel of 451 kinase targets (including 392 wild-type kinases). The size of the red circle is proportional to the percent of DMSO control, where 0% and 35% of control equals 100% and 65% competition, respectively.

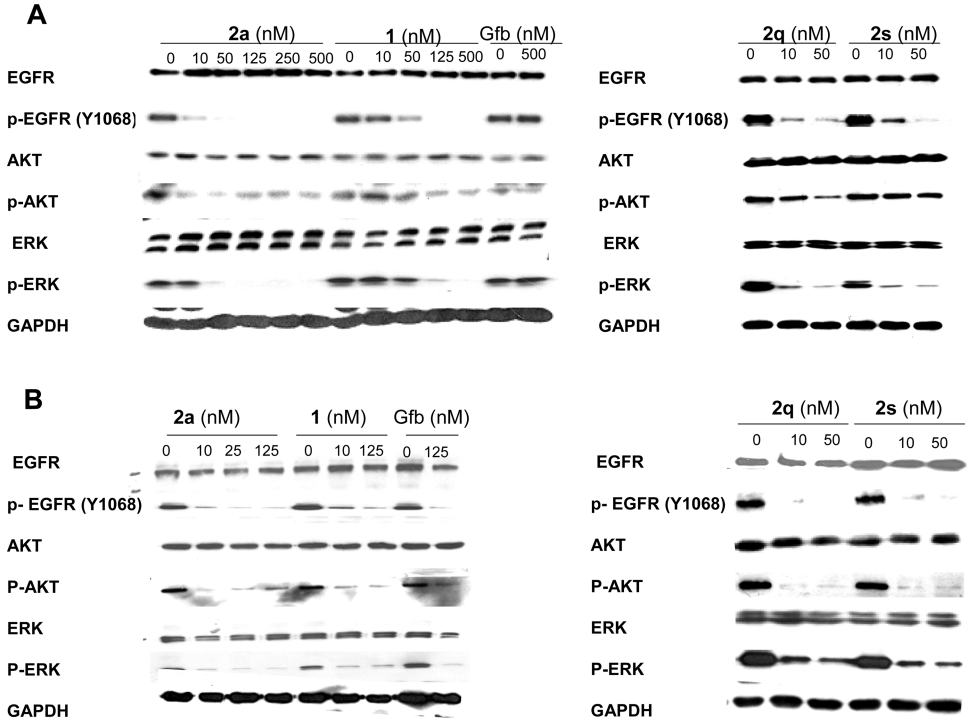

Figure 3. Compounds **2a**, **2q**, and **2s** inhibit the activation of EGFR and downstream signaling in a dose-dependent manner. (A) Compounds **2a**, **2q**, **2s**, and **1** inhibit the activation of EGFR and downstream signaling in H1975 NSCLC cells harboring EGFR$^{L858R/T790M}$, while gefitinib has no effects. (B) Compounds **2a**, **2q**, **2s**, **1**, and gefitinib inhibit the activation of EGFR and downstream signaling in HCC827 NSCLC cells harboring EGFR$^{del\ E746\text{-}A750}$. The results are representative of experiments in triplicate. Gfb: gefitinib.

while compound **2q** also showed strong binding with BMX, FRK, JAK3, KIT^{V559D}, LCK, MAP3K15, PDGFRβ, TEC, and TNK2 at the same time.

In order to further validate the activities of these new EGFR inhibitors, we examined the effects of representative compounds **2a**, **2q**, and **2s** on the activation of EGFR and the downstream signal in cancer cells harboring a different status of EGFR kinases, and the results are summarized in Figure 3. Similar to that of compound **1**, inhibitors **2a**, **2q**, and **2s** dose-dependently inhibited the phosphorylation of EGFR in both H1975 NSCLC cells bearing EGFR$^{L858R/T790M}$ and HCC827 cells harboring EGFR$^{del\ E746\text{-}A750}$.[23] The protein levels of

dx.doi.org/10.1021/jm201591k | *J. Med. Chem.* 2012, 55, 2711−2723

Table 2. Antiproliferative Activities of the Conformation-Constrained Inhibitors 2 against Cells Harboring a Different Status of EGFR[a]

	IC_{50} (μM)				
compound	HCC827 (Del E746_A750)	H1975 (L858R/T790M)	A431 (WT, overexpression)	A549 (WT, *k-Ras* mutation)	HL7702 (WT)
1	0.007 ± 0.001	0.048 ± 0.005	1.39 ± 0.28	5.31 ± 0.56	2.73 ± 0.23
2a	0.018 ± 0.007	0.047 ± 0.014	0.75 ± 0.21	15.94 ± 1.64	>10
2b	0.74 ± 0.08	0.54 ± 0.08	5.62 ± 1.35	>20	>10
2c	0.170 ± 0.006	0.61 ± 0.05	5.06 ± 0.66	12.02 ± 1.21	>10
2d	0.13 ± 0.04	0.15 ± 0.01	>10	10.46 ± 2.08	>10
2e	0.073 ± 0.008	0.72 ± 0.02	2.15 ± 0.48	>20	>10
2f	0.15 ± 0.05	0.53 ± 0.08	1.39 ± 0.48	14.50 ± 1.76	>10
2g	0.044 ± 0.01	0.17 ± 0.02	6.90 ± 1.57	18.02 ± 0.51	>10
2h	6.92 ± 3.32	20.07 ± 1.65	>10	>20	>10
2i	0.014 ± 0.009	0.045 ± 0.017	0.55 ± 0.07	11.35 ± 0.63	7.56 ± 1.83
2j	0.041 ± 0.018	0.024 ± 0.001	0.36 ± 0.17	3.33 ± 0.71	>10
2k	0.014 ± 0.004	0.103 ± 0.002	1.08 ± 0.18	10.35 ± 1.59	>10
2l	0.027 ± 0.001	0.23 ± 0.01	2.11 ± 0.66	11.67 ± 2.15	>10
2m	0.031 ± 0.015	0.20 ± 0.03	0.99 ± 0.30	11.92 ± 1.99	>10
2n	5.01 ± 0.33	8.46 ± 1.26	>10	11.13 ± 1.87	7.18 ± 2.65
2o	0.004 ± 0.001	0.058 ± 0.014	0.82 ± 0.13	8.42 ± 2.64	>10
2p	0.009 ± 0.003	0.054 ± 0.020	0.81 ± 0.02	17.90 ± 3.12	>10
2q	0.003 ± 0.001	0.016 ± 0.006	0.11 ± 0.02	2.80 ± 1.35	4.02 ± 2.28
2r	0.006 ± 0.002	0.030 ± 0.013	0.57 ± 0.02	2.41 ± 0.52	3.44 ± 1.31
2s	0.003 ± 0.001	0.014 ± 0.006	0.17 ± 0.03	2.66 ± 0.33	2.39 ± 0.53
2t	0.018 ± 0.006	0.095 ± 0.008	1.21 ± 0.15	2.27 ± 0.11	3.69 ± 2.73
2u	0.014 ± 0.003	0.048 ± 0.019	1.20 ± 0.24	1.77 ± 0.27	>10
2v	0.023 ± 0.001	0.033 ± 0.011	1.15 ± 0.06	2.47 ± 0.60	2.79 ± 1.35
2w	4.89 ± 1.02	>20	>10	11.17 ± 2.17	>10
2x	6.79 ± 2.48	>20	>10	>30	>10
CI-1033	0.001 ± 0.0003	0.064 ± 0.003	0.15 ± 0.09	1.59 ± 0.58	2.30 ± 0.35
gefitinib	0.008 ± 0.004	9.02 ± 1.08	2.15 ± 0.15	10.21 ± 2.43	>10

[a]The antiproliferative activities of the compounds were evaluated using the MTS assay. The data were means from at least four independent experiments.

downstream p-Akt and p-Erk were also obviously decreased, while the total protein levels of EGFR, Akt, Erk, and GAPDH remained unchanged. Although gefitinib could potently induce the inhibition of EGFR activation and downstream signaling in HCC827 cells, it did not show an effect on the $EGFR^{T790M}$-mutated H1975 cells. The effects of **2a**, **2q**, and **2s** on cells harboring wild type EGFR kinase (EGFR overexpressed A431[24] cells and A549[25] cells bearing *k-Ras* mutation) were also investigated. The results demonstrated that the compounds only moderately affected the activation of EGFR in the corresponding cells although they displayed strong inhibition against EGFR kinase under the in vitro screening assay (Table 1 and Supporting Information).

The antiproliferative effects of the new inhibitors were also investigated to monitor their potential antitumor activities (Table 2). Highly consistent with their strong kinase inhibition, the compounds displayed great antiproliferative effects on HCC827 and H1975 NSCLC cells harboring $EGFR^{del\ E746\text{-}A750}$ and $EGFR^{L858R/T790M}$, respectively. Most of the compounds potently suppressed the growth of HCC827 cancer cells with IC_{50} values in the low nanomolar ranges. Compounds **2o**, **2p**, **2q**, **2r**, and **2s** were equal in potency to that of gefitinib, CI-1033, and **1** for inhibiting the growth of HCC827 cancer cells, with IC_{50} values of 3−9 nM. Moreover, several compounds also displayed strong antiproliferative effects on gefitinib-resistant H1975 cells bearing $EGFR^{L858R/T790M}$. Compounds **2a**, **2i**, **2j**, **2o**, **2p**, **2r**, **2u**, and **2v** were almost equal in potency to that of CI-1033 and inhibitor **1**, while **2q** and **2s** displayed potencies 3−4 times greater than that of **1** against H1975 cancer cell growth. Further investigation also revealed that the compounds **2q** and **2s** potently induced G1 phase arrest and apoptosis in both HCC827 and H1975 NSCLC cells and inhibited the colony formation of H1975 cancer cells in dose-dependent manners (Supporting Information). Not surprisingly, the enzymatically inactive compounds **2n**, **2w**, and **2x** did not show obvious inhibition on the growth of HCC827 or H1975 cancer cells.

Although the compounds also strongly inhibited the enzymatic activity of $EGFR^{WT}$, they were obviously less potent to suppress the proliferation of A431 human epithelial carcinoma cells with overexpressed $EGFR^{WT}$, which might be due to the complex genomic background and the strong binding of $EGFR^{WT}$ with ATP.[31] For instance, compound **2s** inhibited the enzymatic activities of $EGFR^{WT}$, $EGFR^{L858R}$, $EGFR^{L861Q}$, and $EGFR^{L858R/T790M}$, with IC_{50} values of 0.29, 0.67, 0.38, 0.72, and 0.93 nM, respectively. It also potently inhibited the growth of HCC827 and H1975, with IC_{50} values of 3 and 14 nM, but its activity on A431 cancer cells was approximate 10−50 times less potent (IC_{50} value was about 170 nM). However, an irreversible clinical candidate CI-1033 displayed comparable potency to inhibit the growth of H1975 and A431 cancer cells. Similar to many other reversible and irreversible EGFR inhibitors, the compounds only showed moderate inhibitory activities against the growth of A549 NSCLC cells which possess $EGFR^{WT}$ and the *k-Ras* mutation-activating bypass MAPK signal pathway.[28]

Our data have demonstrated that the new EGFR inhibitors also strongly inhibited $EGFR^{WT}$. Because many tissues use wild-type EGFR for normal cellular processes, the potential for toxicity from irreversible EGFR inhibitors is a concern. Therefore, the growth inhibitory activities of the compounds against HL-7702 normal human liver cells which bear $EGFR^{WT}$ were also evaluated to monitor the potential toxic effects.[26] As shown in Table 2, only a few very potent EGFR inhibitors displayed moderate inhibitory activities against the growth of HL-7702 cells, indicating that the cytotoxic effects of these compounds were minimal. For instance, the highly potent inhibitors **2q** and **2s** inhibited the growth of HL-7702 cells with IC_{50} values of 4.02 and 2.39 μM, respectively, which was approximately 200−1000 fold less potent than their activities against the HCC827 and H1975 NSCLC cells. The compounds also displayed moderate or minimal cytotoxicity on human HLF-1 cells (diploid human lung fibroblasts),[27] which further suggested that the compounds might possess a high safety index (Supporting Information).

Given its high potency and remarkable selectivity profile, compound **2s** was further evaluated for in vivo antitumor efficacy in an $EGFR^{L858R/T790M}$-driven human NSCLC xenograft mouse model of H1975 (Figure 4). SCID mice bearing established H1975 tumor xenografts were dosed orally with **2s** at 10 and 30 mg/kg daily (qd) over a 14-day period. Gefitinib (50 mg/kg, qd) was used as a reference drug to validate the resistant models. Both doses of **2s** were well tolerated, with no mortality or significant body weight loss (<5% relative to the vehicle matched controls) observed during the treatment. Dosing at 10 mg/kg/day of **2s** had little effect on the tumor growth compared with the control group. However, compound **2s** displayed significant in vivo antitumor efficacy ($p < 0.05$) and induced tumor stasis at 30 mg/kg/day, indicating that it might serve as a promising lead compound for further development of EGFR inhibitors to overcome $EGFR^{T790M}$ mutation-related clinical resistance to gefitinib or erotinib.

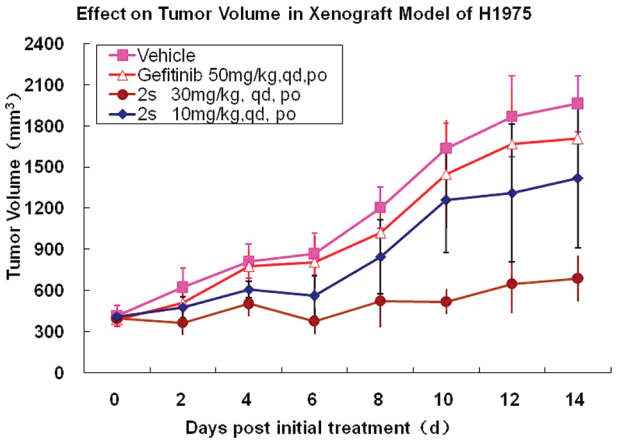

Figure 4. In vivo antitumor effect of compound **2s** in a human NSCLC (H1975) xenograft nude mouse model. The H1975 model was resistant to gefitinib. Mice were monitored for signs of morbidity (behavior and body loss), and tumors were measured every other day. Statistical significance ($p < 0.05$) for antitumor efficacy, based upon tumor growth relative to the vehicle controls. Two animals died at day 10 and 12 in the vehicle control group, respectively.

In summary, a series of 2-oxo-3,4-dihydropyrimido[4,5-*d*]pyrimidinyl derivatives have been designed and synthesized as novel EGFR inhibitors. The compounds potently inhibited the enzymatic activities of different mutants of EGFR as well as the wild type EGFR kinase. The most potent compounds **2q** and **2s** displayed good potencies, with IC_{50} values in the high picomolar range against all types of EGFR kinase, including the clinical resistance-related $EGFR^{T790M}$ mutant. A further kinase profiling study also suggested that the compounds displayed remarkable selectivity on EGFR. The kinase inhibitory efficiencies of the compounds were further validated by Western blot analysis of the activation of EGFR and the downstream signaling in cancer cells harboring different mutants of EGFR. Furthermore, the compounds also strongly inhibited HCC827 and H1975 non small cell lung cancer cells bearing $EGFR^{del\ E746\text{-}A750}$ and $EGFR^{L858R/T790M}$, respectively, with potencies better than that of **1** and CI-1033. The compounds only showed moderate or minimal cytotoxicity to normal HL-7702 and HLF-1 cells, indicating that they might possess a high safety index. Moreover, a further in vivo antitumor efficacy study demonstrated that compound **2s** significantly inhibited the tumor growth and induced tumor stasis in an $EGFR^{L858R/T790M}$-driven human NSCLC xenograft mouse model of H1975 by orally dosing at 30 mg/kg/day. Our study provides a new lead compound with a different chemical scaffold for further development of EGFR inhibitors to overcome $EGFR^{T790M}$ mutation-related clinical resistance to gefitinib or erotinib. Further extensive pharmacokinetics and safety evaluation on **2s** are in progress and will be reported in due course.

EXPERIMENTAL SECTION

Chemistry. Reagents and solvents were obtained from commercial suppliers and used without further purification. Flash chromatography was performed using silica gel (300−400 mesh). All reactions were monitored by TLC, using silica gel plates with fluorescence F_{254} and UV light visualization. ^1H and ^{13}C NMR spectra were recorded on a Bruker AV-400 spectrometer at 400 MHz and Bruker AV-500 spectrometer at 125 MHz, respectively. Coupling constants (J) are expressed in hertz (Hz). Chemical shifts (δ) of NMR are reported in parts per million (ppm) units relative to internal control (TMS). The low or high resolution of ESI-MS was recorded on an Agilent 1200 HPLC-MSD mass spectrometer or Applied Biosystems Q-STAR Elite ESI-LC-MS/MS mass spectrometer, respectively. The purity of compounds was determined by reverse-phase high performance liquid chromatography (HPLC) analysis to be over 95% (>95%). HPLC instrument: Dionex Summit HPLC (Column: Diamonsil C18, 5.0 μm, 4.6 × 250 mm (Dikma Technologies); detector: PDA-100 photodiode array; injector: ASI-100 autoinjector; pump: p-680A). Elution: MeOH in water; flow rate: 1.0 mL/min.

*Ethyl 4-(3-(tert-Butoxycarbonylamino)phenylamino)-2-(methylthio)pyrimidine-5-carboxylate (**5**).* To a solution of compound **4** (20.8 g, 100 mmol) in DMF (300 mL) were added potassium carbonate (27.6 g, 200 mmol) and compound **3** (23.3 g, 100 mmol). The reaction was heated to 80 °C and stirred overnight. After being cooled to room temperature, the reaction mixture was added to ice−water (1000 mL). The precipitate was filtered, and the filtered cake was rinsed with additional cool water and dried in a vacuum oven to give the title compound (38.8 g, 96% yield), which was used without further purification. ^1H NMR (400 MHz, $CDCl_3$) δ 10.37 (s, 1H), 8.76 (s, 1H), 7.90 (s, 1H), 7.34 (d, J = 8.0 Hz, 1H), 7.24 (t, J = 8.0 Hz, 1H), 7.02 (d, J = 8.0 Hz, 1H), 6.53 (s, 1H), 4.38 (q, J = 7.2, 14.4 Hz, 2H), 2.55 (s, 3H), 1.52 (s, 9H), 1.40 (t, J = 7.2 Hz, 3H).

*tert-Butyl 3-(5-(Hydroxymethyl)-2-(methylthio)pyrimidin-4-ylamino)phenylcarbamate (**6**).* To a solution of compound **5** (20.2 g, 50 mmol) in THF (500 mL) was added 2.0 M lithium aluminum hydride solution in THF (50 mL, 100 mmol) at −40 °C. The reaction mixture was stirred until the temperature warmed to room temperature and was then treated with saturated NH_4Cl solution (75 mL). After the mixture was stirred at room temperature for 30

min, the solid was filtered off. The filtrate was partitioned between dichloromethane (500 mL) and water (300 mL). The organic layer was washed with brine and dried over Na_2SO_4, the solid was filtered off, and the filtrate was concentrated under reduced pressure. The resulting crude product was purified by flash silica gel chromatography with dichloromethane/methanol (80/1 to 40/1, v/v) to yield the title product as a white solid (10.33 g, 57%). ^{1}H NMR (400 MHz, $CDCl_3$) δ 8.02 (s, 1H), 7.86 (s, 1H), 7.80 (s, 1H), 7.36 (dd, J = 1.2, 8.0 Hz, 1H), 7.22 (t, J = 8.0 Hz, 1H), 6.95 (dd, J = 1.2, 8.0 Hz, 1H), 6.52 (s, 1H), 4.61 (s, 2H), 2.52 (s, 3H), 1.52 (s, 9H).

*tert-Butyl 3-(5-Formyl-2-(methylthio)pyrimidin-4-ylamino)-phenylcarbamate (**7**).* To a solution of compound **6** (10.0 g, 27.6 mmol) in dichloromethane (300 mL) was added activated manganese-(IV) oxide (24.0 g, 276 mmol) at room temperature, and the mixture was stirred overnight, the solid was filtered off, and the filtrate was concentrated under reduced pressure. The resulting crude product was purified by flash silica gel chromatography with petroleum ether/ethyl acetate (5/1 to 3/1, v/v) to yield the title product as a white solid (8.36 g, 84%). ^{1}H NMR (400 MHz, $CDCl_3$) δ 10.61 (s, 1H), 9.77 (s, 1H), 8.43 (s, 1H), 7.98 (s, 1H), 7.36 (dd, J = 0.8, 8.0 Hz, 1H), 7.25–7.29 (m, 1H), 7.03 (dd, J = 1.2, 8.0 Hz, 1H), 6.51 (s, 1H), 2.59 (s, 3H), 1.53 (s, 9H).

*tert-Butyl 3-(5-((Methylamino)methyl)-2-(methylthio)pyrimidin-4-ylamino)phenylcarbamate (**8a**).* To a solution of compound 7 (7.21 g, 20.0 mmol) in methanol (200 mL) were added sodium acetate (8.2 g, 100 mmol) and methanaminium chloride (6.75 g, 100 mmol) at room temperature, and the mixture was stirred for 1 h. $NaBH_4$ (1.51 g, 40.0 mmol) was added. The reaction mixture was partitioned between dichloromethane (200 mL) and saturated $NaHCO_3$ (100 mL), and then the water layer was extracted with dichloromethane (100 mL × 2). The combined organic layer was washed with brine and dried over Na_2SO_4, the solid was filtered off, and the filtrate was concentrated under reduced pressure. The resulting crude product was purified by silica gel chromatography with dichloromethane/methanol (80/1 to 40/1, v/v) to give the title product as a white solid (5.25 g, 71%). ^{1}H NMR (400 MHz, $CDCl_3$) δ 10.12 (s, 1H), 7.89 (s, 1H), 7.78 (s, 1H), 7.35 (d, J = 8.8 Hz, 1H), 7.21 (t, J = 8.0 Hz, 1H), 6.97 (dd, J = 1.2, 8.0 Hz, 1H), 6.50 (s, 1H), 3.74 (s, 2H), 3.55 (s, 3H), 2.44 (s, 3H), 1.52 (s, 9H).

*tert-Butyl 3-(3-mMethyl-7-(methylthio)-2-oxo-3,4-dihydropyrimido[4,5-d]pyrimidin-1(2H)-yl)phenylcarbamate (**9a**).* To a solution of compound **8a** (5.20 g, 13.8 mmol) in THF (140 mL) were added DIEA (8 mL, 55.2 mmol) and 0.2 M triphosgene (25 mL, 5.05 mmol) at 0 °C, and the mixture was stirred at room temperature for 1 h and then partitioned between dichloromethane (200 mL) and saturated $NaHCO_3$ (100 mL) solution. The organic layer was washed with brine and dried over Na_2SO_4, the solid was filtered off, and the filtrate was concentrated under reduced pressure. The resulting crude product was purified by silica gel chromatography with dichloromethane/methanol (60/1 to 30/1, v/v) to give the title product as a white solid (4.71 g, 85%). ^{1}H NMR (400 MHz, $CDCl_3$) δ 8.10 (s, 1H), 7.44 (s, 1H), 7.34 (t, J = 8.0 Hz, 1H), 7.23 (d, J = 7.2 Hz, 1H), 6.90 (d, J = 8.0 Hz, 1H), 6.55 (s, 1H), 4.46 (s, 2H), 3.08 (s, 3H), 2.14 (s, 3H), 1.50 (s, 9H).

*tert-Butyl 3-(3-Methyl-7-(methylsulfonyl)-2-oxo-3,4-dihydropyrimido[4,5-d]pyrimidin-1(2H)-yl)phenylcarbamate (**10a**).* To a solution of compound **9a** (4.0 g, 10.0 mmol) in dichloromethane (100 mL) was added 85% *m*-chloroperbenzoic acid (6.1 g, 30.0 mmol) in batches at 0 °C. The reaction mixture was stirred for 3 h at room temperature. The reaction mixture was partitioned between dichloromethane (200 mL) and saturated $NaHCO_3$ (100 mL). The organic layer was washed with brine and dried over Na_2SO_4, the solid was filtered off, and the filtrate was concentrated under reduced pressure. The resulting white solid (3.90 g, 90% yield) was recrystallized from a minimum amount of ethyl acetate, which was used for the next step without further purification. ^{1}H NMR (400 MHz, $CDCl_3$) δ 8.45 (s, 1H), 7.58 (s, 1H), 7.35 (t, J = 8.0 Hz, 1H), 7.15 (dd, J = 1.2, 8.0 Hz, 1H), 6.89 (dd, J = 1.2, 8.0 Hz, 1H), 6.67 (s, 1H), 4.62 (s, 2H), 3.11 (s, 3H), 2.98 (s, 3H), 1.48 (s, 9H).

*tert-Butyl 3-(7-(2-Methoxy-4-(4-methylpiperazin-1-yl)-phenylamino)-3-methyl-2-oxo-3,4-dihydropyrimido[4,5-d]-pyrimidin-1(2H)-yl)phenylcarbamate (**11a**).* To a solution of compound **10a** (260 mg, 0.6 mmol) in butan-2-ol (2 mL) were added 2-methoxy-4-(4-methylpiperazin-1-yl)aniline (133 mg, 0.6 mmol) and trifluoroacetic acid (48 μL, 0.6 mmol). The reaction mixture was stirred for 18 h at 110 °C in a sealed tube. The reaction mixture was cooled to room temperature and partitioned between dichloromethane (30 mL) and saturated $NaHCO_3$ (10 mL), and the water layer was extracted with dichloromethane (10 mL × 2). The combined organic layer was washed with brine and dried with Na_2SO_4, the solid was filtered off, and the filtrate was concentrated under reduced pressure. The resulting crude product was purified by silica gel chromatography with dichloromethane/methanol (40/1 to 20/1, v/v) to give the title product as a yellow solid (151 mg, 44%). ^{1}H NMR (400 MHz, $CDCl_3$) δ 7.99 (s, 1H), 7.48 (d, J = 7.5 Hz, 1H), 7.44 (s, 1H), 7.41 (t, J = 8.0 Hz, 1H), 7.35 (s, 1H), 6.97 (d, J = 7.5 Hz, 1H), 6.63 (s, 1H), 6.42 (d, J = 2.0 Hz, 1H), 6.16 (d, J = 6.4 Hz, 1H), 4.42 (s, 2H), 3.80 (s, 3H), 3.22 (m, 4H), 3.08 (s, 3H), 2.79 (m, 4H), 1.47 (s, 9H). LCMS (ESI): m/z 575.3 $[M + H]^+$.

*1-(3-Aminophenyl)-7-(2-methoxy-4-(4-methylpiperazin-1-yl)-phenylamino)-3-methyl-3,4-dihydropyrimido[4,5-d]pyrimidin-2(1H)-one (**2w**).* To a solution of compound **11a** (143 mg, 0.25 mmol) in dichloromethane (1 mL) was added trifluoroacetic acid (0.2 mL, 2.7 mmol). The reaction mixture was stirred for 1 h at room temperature. The reaction mixture was cooled to room temperature and partitioned between dichloromethane (10 mL) and saturated $NaHCO_3$ (2 mL), and the water layer was extracted with dichloromethane (5 mL × 2). The combined organic layer was washed with brine and dried with Na_2SO_4, the solid was filtered off, and the filtrate was concentrated under reduced pressure. The resulting crude product was purified by silica gel chromatography with dichloromethane/methanol (40/1 to 20/1, v/v) to give the title product as a yellow solid (100 mg, 84%). ^{1}H NMR (400 MHz, $CDCl_3$) δ 7.99 (s, 1H), 7.61 (s, 1H), 7.46 (s, 1H), 7.28 (t, J = 8.0 Hz, 2H), 6.78 (dd, J = 2.0, 8.0 Hz, 1H), 6.67 (d, J = 7.6 Hz, 1H), 6.61 (t, J = 2.0 Hz, 1H), 6.45 (d, J = 2.4 Hz, 1H), 6.21 (d, J = 7.6 Hz, 1H), 4.42 (s, 2H), 3.81 (s, 3H), 3.13 (t, J = 4.8 Hz, 4H), 3.09 (s, 3H), 2.64 (t, J = 4.8 Hz, 4H), 2.29 (s, 3H). LCMS (ESI): m/z 475.2 $[M + H]^+$.

*N-(3-(7-(2-Methoxy-4-(4-methylpiperazin-1-yl)phenylamino)-3-methyl-2-oxo-3,4-dihydropyrimido[4,5-d]pyrimidin-1(2H)-yl)-phenyl)acrylamide (**2a**).* To a solution of compound **2x** (95 mg, 0.20 mmol) in dichloromethane (2 mL) were added diisopropyethylamine (40 μL, 0.20 mmol) and acryloyl chloride (16 μL, 0.20 mmol). The reaction mixture was stirred for 1 h at room temperature. The resulting crude product was purified by silica gel chromatography with dichloromethane/methanol (40/1 to 20/1, v/v) to give the title product as a yellow solid (90 mg, 85%). ^{1}H NMR (400 MHz, DMSO-d_6) δ 10.31 (s, 1H), 8.11 (s, 1H), 7.81 (d, J = 7.6 Hz, 1H), 7.56 (s, 1H), 7.48 (s, 1H), 7.43 (t, J = 8.0 Hz, 1H), 7.27 (d, J = 8.4 Hz, 1H), 6.95 (d, J = 8.0 Hz, 1H), 6.51 (s, 1H), 6.44 (dd, J = 10.0, 16.8 Hz, 1H), 6.25 (d, J = 16.8 Hz, 1H), 6.02 (d, J = 8.0 Hz, 1H), 5.76 (d, J = 10.0 Hz, 1H), 4.46 (s, 2H), 3.76 (s, 3H), 2.99 (m, 4H), 2.96 (s, 3H), 2.50 (m, 4H), 2.22 (s, 3H). ^{13}C NMR (125 MHz, DMSO-d_6) δ 163.12, 158.45, 157.23, 154.03, 152.54, 146.70, 139.52, 137.49, 131.76, 128.92, 126.92, 124.92, 120.79, 120.72, 118.24, 106.41, 101.15, 99.75, 55.61, 54.59, 48.72, 45.82, 45.70, 34.99. HRMS (ESI): exact mass calcd for $C_{28}H_{32}N_8O_3$ $[M + H]^+$, 529.2670, found 529.2675.

The following compounds (**2b–x**) were prepared from compound **10** and the corresponding aniline by a method similar to that for **2a**.

*N-(3-(7-(4-(Dimethylamino)-2-methoxyphenylamino)-3-methyl-2-oxo-3,4-dihydropyrimido[4,5-d]pyrimidin-1(2H)-yl)phenyl)-acrylamide (**2b**).* ^{1}H NMR (400 MHz, DMSO-d_6) δ 10.28 (s, 1H), 8.09 (s, 1H), 7.79 (d, J = 8.8 Hz, 1H), 7.57 (s, 1H), 7.42 (t, J = 8.0 Hz, 2H), 7.22 (d, J = 8.8 Hz, 1H), 6.95 (d, J = 8.0 Hz, 1H), 6.43 (dd, J = 10.0, 16.8 Hz, 1H), 6.30 (d, J = 2.4 Hz, 1H), 6.25 (dd, J = 2.0, 16.8 Hz, 1H), 5.87 (d, J = 7.6 Hz, 1H), 5.75 (dd, J = 2.0, 10.0 Hz, 1H), 4.45 (s, 2H), 3.76 (s, 3H), 2.96 (s, 3H), 2.78 (s, 6H). ^{13}C NMR (125 MHz, DMSO-d_6) δ163.12, 158.42, 157.20, 153.98, 152.58, 146.82, 139.51, 137.51, 131.76, 128.85, 126.91, 124.93, 120.70, 118.59, 118.16, 103.81,

100.82, 96.77, 55.48, 45.81, 40.58, 34.98. HRMS (ESI): exact mass calcd for $C_{25}H_{27}N_7O_3$ $[M + H]^+$, 474.2248, found 474.2252.

*N-(3-(7-(2-Methoxy-4-(piperidin-1-yl)phenylamino)-3-methyl-2-oxo-3,4-dihydropyrimido[4,5-d]pyrimidin-1(2H)-yl)phenyl)-acrylamide (**2c**).* ^{1}H NMR (400 MHz, DMSO-d_6) δ 10.30 (s, 1H), 8.11 (s, 1H), 7.82 (d, J = 8.0 Hz, 1H), 7.56 (s, 1H), 7.47 (s, 1H), 7.43 (t, J = 8.0 Hz, 1H), 7.25 (d, J = 8.0 Hz, 1H), 6.95 (d, J = 8.0 Hz, 1H), 6.49 (d, J = 2.2 Hz, 1H), 6.43 (dd, J = 8.0, 16.0 Hz, 1H), 6.25 (dd, J = 1.6, 8.0 Hz, 1H), 6.02 (d, J = 7.4 Hz, 1H), 5.76 (dd, J = 1.6, 8.0 Hz, 1H), 4.46 (s, 2H), 3.75 (s, 3H), 2.96 (m, 7H), 1.59 (m, 4H), 1.49−1.504 (m, 2H). ^{13}C NMR (125 MHz, DMSO-d_6) δ163.57, 158.70, 157.68, 154.48, 153.00, 148.08, 139.99, 137.95, 132.20, 129.37, 127.36, 125.37, 121.15, 118.63, 107.50, 101.56, 100.87, 56.02, 50.90, 46.27, 35.44, 25.82, 24.30. HRMS (ESI): exact mass calcd for $C_{28}H_{31}N_7O_3$ $[M + H]^+$, 514.2561, found 514.2565.

*N-(3-(7-(2-Methoxy-4-morpholinophenylamino)-3-methyl-2-oxo-3,4-dihydropyrimido[4,5-d]pyrimidin-1(2H)-yl)phenyl)-acrylamide (**2d**).* ^{1}H NMR (400 MHz, DMSO-d_6) δ 10.30 (s, 1H), 8.12 (s, 1H), 7.81 (d, J = 6.8 Hz, 1H), 7.56 (s, 1H), 7.50 (s, 1H), 7.43 (t, J = 8.0 Hz, 1H), 7.28 (d, J = 10.0 Hz, 1H), 6.96 (d, J = 10.0 Hz, 1H), 6.52 (d, J = 2.0 Hz, 1H), 6.43 (dd, J = 10.0, 16.8 Hz, 1H), 6.22−6.27 (m, 1H), 6.02 (d, J = 8.0 Hz, 1H), 5.74−5.77 (m, 1H), 4.46 (s, 2H), 3.76 (s, 3H), 3.71 (t, J = 4.4 Hz, 4H), 2.96 (m, 7H). ^{13}C NMR (125 MHz, DMSO-d_6) δ 163.58, 158.68, 157.68, 154.49, 152.98, 147.23, 139.96, 137.95, 132.20, 129.38, 127.42, 125.39, 121.56, 121.19, 118.71, 106.61, 101.65, 100.02, 66.53, 56.09, 49.66, 46.27, 35.44. HRMS (ESI): exact mass calcd for $C_{27}H_{29}N_7O_4$ $[M + H]^+$, 516.2354, found 516.2358.

*N-(3-(7-(2-Methoxy-4-(4-methyl-1,4-diazepan-1-yl)-phenylamino)-3-methyl-2-oxo-3,4-dihydropyrimido[4,5-d]-pyrimidin-1(2H)-yl)phenyl)acrylamide (**5e**).* ^{1}H NMR (400 MHz, DMSO-d_6) δ 10.30 (s, 1H), 8.19 (s, 1H), 7.85 (s, 1H), 7.69−7.70 (m, 2H), 7.51 (t, J = 8.0 Hz, 1H), 7.45 (t, J = 8.0 Hz, 1H), 6.96−6.99 (m, 2H), 6.40−6.46 (m, 2H), 6.24 (dd, J = 1.6, 16.8 Hz, 1H), 5.75 (dd, J = 1.6, 10.0 Hz, 1H), 4.50 (s, 2H), 3.33 (m, 7H), 2.98 (s, 3H), 2.74 (t, J = 4.4 Hz, 4H), 2.49 (m, 2H), 2.24 (s, 3H). ^{13}C NMR (125 MHz, DMSO-d_6) δ 163.11, 158.51, 157.21, 154.01, 152.63, 149.63, 139.54, 137.55, 131.77, 128.88, 126.93, 124.94, 120.69, 118.14, 117.40, 102.43, 100.64, 95.24, 57.14, 56.31, 55.45, 48.25, 47.90, 46.01, 45.84, 35.00, 26.93. HRMS (ESI): exact mass calcd for $C_{29}H_{34}N_8O_3$ $[M + H]^+$, 543.2827, found 543.2832.

*N-(3-(7-(4-(4-(Dimethylamino)piperidin-1-yl)-2-methoxyphenylamino)-3-methyl-2-oxo-3,4-dihydropyrimido[4,5-d]pyrimidin-1(2H)-yl)phenyl)acrylamide (**5f**).* ^{1}H NMR (400 MHz, DMSO-d_6) δ 10.34 (s, 1H), 8.11 (s, 1H), 7.84 (d, J = 7.6 Hz, 1H), 7.55 (s, 1H), 7.48 (s, 1H), 7.42 (t, J = 8.0 Hz, 1H), 7.25 (d, J = 8.4 Hz, 1H), 6.95 (d, J = 7.2 Hz, 1H), 6.51 (s, 1H), 6.45 (dd, J = 10.0, 17.2 Hz, 1H), 6.25 (d, J = 16.8 Hz, 1H), 6.04 (s, 1H), 5.76 (d, J = 9.6 Hz, 1H), 4.46 (s, 2H), 3.75 (s, 3H), 3.56 (d, J = 12.4 Hz, 2H), 3.35 (s, 3H), 2.87 (m, 1H), 2.49−2.56 (m, 2H), 2.34 (s, 6H), 1.86 (d, J = 10.4 Hz, 2H), 1.46−1.55 (m, 2H). ^{13}C NMR (125 MHz, DMSO-d_6) δ163.12, 158.24, 157.23, 154.04, 152.54, 146.93, 139.54, 137.50, 131.77, 128.91, 126.90, 124.92, 120.71, 120.65, 118.20, 106.98, 101.12, 100.32, 61.37, 55.59, 48.87, 45.83, 41.45, 34.99, 27.85. HRMS (ESI): exact mass calcd for $C_{30}H_{36}N_8O_3$ $[M + H]^+$, 557.2983, found 557.2989.

*N-(3-(3-Methyl-2-oxo-7-(phenylamino)-3,4-dihydropyrimido[4,5-d]pyrimidin-1(2H)-yl)phenyl)acrylamide (**2g**).* ^{1}H NMR (400 MHz, DMSO-d_6) δ 10.30 (s, 1H), 9.41 (s, 1H), 8.18 (s, 1H), 7.43 (d, J = 8.0 Hz, 1H), 7.66 (s, 1H), 7.45 (t, J = 8.0 Hz, 1H), 7.27 (d, J = 8.0 Hz, 2H), 6.99 (d, J = 8.0 Hz, 1H), 6.93 (t, J = 7.6 Hz, 2H), 6.75 (t, J = 7.2 Hz, 1H), 6.42 (dd, J = 10.4, 16.8 Hz, 1H), 6.24(d, J = 16.8 Hz, 1H), 5.75 (d, J = 10.4 Hz, 1H), 4.48 (s, 2H), 2.97 (s, 3H). ^{13}C NMR (125 MHz, DMSO-d_6) δ163.14, 158.32, 157.17, 154.05, 152.52, 140.33, 139.59, 137.66, 131.70, 128.94, 127.93, 127.00, 125.06, 120.75, 120.67, 118.26, 118.05, 101.39, 45.87, 34.99. HRMS (ESI): exact mass calcd for $C_{22}H_{20}N_6O_2$ $[M + H]^+$, 401.1721, found 401.1735.

*N-(3-(3-Methyl-7-(methylamino)-2-oxo-3,4-dihydropyrimido[4,5-d]pyrimidin-1(2H)-yl)phenyl)acrylamide (**2h**).* ^{1}H NMR (400 MHz, DMSO-d_6) δ 10.23 (s, 1H), 8.01 (s, 1H), 7.61 (d, J = 8.0 Hz, 1H), 7.55 (s, 1H), 7.36 (t, J = 8.0 Hz, 1H), 6.91 (d, J = 7.6 Hz, 1H), 6.71 (s, 1H), 6.43 (dd, J = 10.0, 16.8 Hz, 1H), 6.25 (d, J = 16.8 Hz, 1H), 5.76 (d, J = 10.4 Hz, 1H), 4.37 (s, 2H), 2.93 (s, 3H), 2.59 (s, 3H). ^{13}C NMR (125 MHz, DMSO-d_6) δ 163.11, 161.56, 157.11, 153.74, 152.93, 139.14, 137.44,131.75, 128.50, 126.92, 125.14, 120.87, 118.23, 45.68, 35.01. HRMS (ESI): exact mass calcd for $C_{17}H_{18}N_6O_2$ $[M + H]^+$, 339.1564, found 339.1566.

*N-(3-(3-Methyl-7-(4-(4-methylpiperazin-1-yl)phenylamino)-2-oxo-3,4-dihydropyrimido[4,5-d]pyrimidin-1(2H)-yl)phenyl)-acrylamide (**2i**).* ^{1}H NMR (400 MHz, DMSO-d_6) δ 10.31 (s, 1H), 9.17 (s, 1H), 8.13 (s, 1H), 7.84 (d, J = 8.0 Hz, 1H), 7.56 (s, 1H), 7.44 (t, J = 8.0 Hz, 1H), 7.12 (d, J = 7.2 Hz, 2H), 6.96 (d, J = 7.6 Hz, 1H), 6.53 (d, J = 8.0 Hz, 2H), 6.43 (dd, J = 9.6, 16.4 Hz, 1H), 6.25 (d, J = 16.4 Hz, 1H), 5.76 (d, J = 10.0 Hz, 1H), 4.46 (s, 2H), 2.97 (s, 3H), 2.92 (s, 4H), 2.41 (s, 4H), 2.20 (s, 3H). ^{13}C NMR (125 MHz, DMSO-d_6) δ 163.15, 158.41, 157.12, 154.03, 152.63, 145.53, 139.58, 137.68, 132.69, 131.75, 129.00, 126.99, 124.99, 120.79, 119.07, 118.22, 115.44, 100.58, 54.64, 48.83, 45.77, 35.01. HRMS (ESI): exact mass calcd for $C_{27}H_{30}N_8O_{22}$ $[M + H]^+$, 499.2564, found 499.2562.

*N-(3-(7-(3-Methoxy-4-(4-methylpiperazin-1-yl)phenylamino)-3-methyl-2-oxo-3,4-dihydropyrimido[4,5-d]pyrimidin-1(2H)-yl)-phenyl)acrylamide (**2j**).* ^{1}H NMR (400 MHz, DMSO-d_6) δ 10.30 (s, 1H), 9.13 (s, 1H), 8.15 (s, 1H), 7.79 (d, J = 8.4 Hz, 1H), 7.58 (s, 1H), 7.42 (d, J = 8.0 Hz, 1H), 6.91−6.97 (m, 2H), 6.86 (s, 1H), 6.39−6.46 (m, 2H), 6.24 (d, J = 16.8 Hz, 1H), 5.75 (d, J = 10.0 Hz, 1H), 4.46 (s, 2H), 3.58 (s, 3H), 2.96 (s, 3H), 2.79 (s, 4H), 2.39 (s, 4H), 2.19 (s, 3H). ^{13}C NMR (125 MHz, DMSO-d_6) δ 163.11, 158.46, 157.14, 153.92, 152.64, 151.68, 139.55, 137.55, 135.51, 135.36, 131.74, 128.89, 126.93, 124.95, 120.74, 118.20, 117.34, 110.55, 103.72, 101.06, 55.20, 54.95, 50.18, 45.86, 45.82, 35.01. HRMS (ESI): exact mass calcd for $C_{28}H_{32}N_8O_3$ $[M + H]^+$, 529.2670, found 529.2667.

*N-(3-(7-(2-Ethoxy-4-(4-methylpiperazin-1-yl)phenylamino)-3-methyl-2-oxo-3,4-dihydropyrimido[4,5-d]pyrimidin-1(2H)-yl)-phenyl)acrylamide (**2k**).* ^{1}H NMR (400 MHz, $CDCl_3$) δ 8.28 (s, 1H), 7.99 (s, 1H), 7.93 (d, J = 7.6 Hz, 1H), 7.48 (s, 1H), 7.40 (t, J = 8.0 Hz, 2H), 7.28 (s, 1H), 6.96 (d, J = 8.0 Hz, 1H), 6.38 (s, 1H), 6.34 (d, J = 16.4 Hz, 1H), 6.18 (dd, J = 10.0, 16.8 Hz, 1H), 6.10 (d, J = 8.4 Hz, 1H), 5.65 (d, J = 10.4 Hz, 1H), 4.42 (s, 2H), 4.00 (q, J = 6.8, 13.6 Hz, 2H), 3.13 (s, 4H), 3. 06 (s, 3H), 2.70 (s, 4H), 2.44 (s, 3H), 1.39 (t, J = 6.8 Hz, 3H). ^{13}C NMR (125 MHz, $CDCl_3$) δ 163.39, 158.58, 157.56, 153.72, 147.44, 146.03, 139.35, 137.15, 131.54, 129.63, 127.12, 125.19, 122.57, 121.09, 119.70, 118.94, 108.52, 101.04, 100.11, 64.19, 54.78, 49.44, 46.96, 45.49, 35.62, 14.91. HRMS (ESI): exact mass calcd for $C_{29}H_{34}N_8O_3$ $[M + H]^+$, 543.2827, found 543.2834.

*N-(3-(7-(2-Isopropoxy-4-(4-methylpiperazin-1-yl)phenylamino)-3-methyl-2-oxo-3,4-dihydropyrimido[4,5-d]pyrimidin-1(2H)-yl)-phenyl)acrylamide (**2l**).* ^{1}H NMR (400 MHz, DMSO-d_6) δ 8.40 (s, 1H), 7.96 (s, 1H), 7.91 (d, J = 8.0 Hz, 1H), 7.49 (s, 1H), 7.37 (t, J = 8.0 Hz, 2H), 7.25 (s, 1H), 6.94 (d, J = 7.6 Hz, 1H), 6.41 (d, J = 2.0 Hz, 1H), 6.32 (d, J = 12.8 Hz, 1H), 6.14−6.18 (m, 1H), 6.08−6.11 (m, 1H), 5.62 (d, J = 10.0 Hz, 1H), 4.47−4.53 (m, 1H), 4.39 (s, 2H), 3.05 (t, J = 4.8 Hz, 4H), 3.03 (s, 3H), 2.56 (t, J = 4.6 Hz, 4H), 2.34 (s, 3H), 1.30 (d, J = 6.0 Hz, 6H). ^{13}C NMR (125 MHz, DMSO-d_6) δ 163.39, 158.50, 157.46, 153.70, 146.39, 139.54, 136.95, 131.65, 129.61, 126.83, 124.95, 123.15, 121.02, 119.75, 118.92, 108.52, 102.48, 99.86, 71.26, 55.05, 49.80, 46.94, 45.99, 35.61, 22.19. HRMS (ESI): exact mass calcd for $C_{30}H_{36}N_8O_3$ $[M + H]^+$, 557.2987, found 557.2990.

*N-(3-(3-Methyl-7-(2-methyl-4-(4-methylpiperazin-1-yl)-phenylamino)-2-oxo-3,4-dihydropyrimido[4,5-d]pyrimidin-1(2H)-yl)phenyl)acrylamide (**2m**).* ^{1}H NMR (400 MHz, $CDCl_3$) δ 8.35 (s, 1H), 7.97 (s, 1H), 7.62 (d, J = 7.6 Hz, 1H), 7.45 (s, 1H), 7.27−7.33 (m, 2H), 6.91 (d, J = 8.0 Hz, 1H), 6.64 (s, 1H), 6.56 (s, 1H), 6.49 (d, J = 8.0 Hz, 1H), 6.33 (d, J = 16.8 Hz, 1H), 6.17 (dd, J = 10.0, 16.8 Hz, 1H), 5.64 (d, J = 10.4 Hz, 1H), 4.44 (s, 2H), 3.14 (m, 4H), 3.10 (s, 3H), 2.65 (m, 4H), 2.41 (s, 3H), 2.14 (s, 3H). ^{13}C NMR (125 MHz, $CDCl_3$) δ 163.47, 159.65, 157.61, 153.65, 147.23, 139.42, 136.82, 131.65, 129.92, 129.27, 126.80, 125.04, 121.15, 119.65, 118.22, 114.43, 100.52, 54.90, 49.17, 46.87, 45.69, 35.67, 18.38. HRMS (ESI): exact mass calcd for $C_{28}H_{32}N_8O_2$ $[M + H]^+$, 513.2721, found 513.2719.

*N-(3-(7-(2-Fluoro-4-(4-methylpiperazin-1-yl)phenylamino)-3-methyl-2-oxo-3,4-dihydropyrimido[4,5-d]pyrimidin-1(2H)-yl)-phenyl)acrylamide (**2n**).* ^{1}H NMR (400 MHz, DMSO-d_6) δ 10.30 (s, 1H), 8.19 (s, 1H), 7.86 (s, 1H), 7.69−7.70 (m, 2H), 7.51 (t, J = 8.0

Hz, 1H), 7.45 (t, J = 8.0 Hz, 1H), 6.96−6.99 (m, 2H), 6.40−6.47 (m, 2H), 6.24 (dd, J = 2.0, 17.2 Hz, 1H), 5.75 (dd, J = 2.0, 10.0 Hz, 1H), 4.50 (s, 2H), 2.98 (s, 3H), 2.74 (t, J = 4.4 Hz, 4H), 2.50 (m, 4H), 2.24 (s, 3H). ^{13}C NMR (125 MHz, DMSO-d_6) δ 163.63, 158.28, 158.10, 157.76, 156.37, 154.66, 152.80, 142.47, 142.41, 140.00, 137.93, 132.14, 130.90, 129.41, 127.48, 125.45, 121.17, 118.80, 110.27, 110.10, 108.35, 108.17, 102.59, 55.42, 51.48, 46.28, 45.98, 35.45. HRMS (ESI): exact mass calcd for $C_{27}H_{29}FN_8O_2$ [M + H]$^+$, 517.2470, found 517.2473.

*N-(3-(3-Isopropyl-7-(2-methoxy-4-(4-methylpiperazin-1-yl)-phenylamino)-2-oxo-3,4-dihydropyrimido[4,5-d]pyrimidin-1(2H)-yl)phenyl)acrylamide (**2o**).* ^{1}H NMR (400 MHz, DMSO-d_6) δ 10.32 (s, 1H), 8.14 (s, 1H), 7.80 (d, J = 6.8 Hz, 1H), 7.57 (s, 1H), 7.48 (s, 1H), 7.42 (t, J = 8.0 Hz, 1H), 7.29 (d, J = 7.6 Hz, 1H), 6.97 (d, J = 8.0 Hz, 1H), 6.52 (s, 1H), 6.43 (dd, J = 10.0, 17.2 Hz, 1H), 6.25 (d, J = 16.8 Hz, 1H), 6.04 (d, J = 9.2 Hz, 1H), 5.76 (d, J = 10.4 Hz, 1H), 4.52−4.55 (m, 1H), 4.37 (s, 2H), 3.76 (s, 3H), 3.04 (m, 4H), 2.57 (m, 4H), 2.32 (s, 3H), 1.19 (d, J = 6.8 Hz, 6H). ^{13}C NMR (125 MHz, DMSO-d_6) δ163.11, 158.31, 157.12, 154.03, 152.13, 146.79, 139.44, 137.58, 131.75, 128.85, 126.91, 125.01, 120.80, 118.22, 106.43, 101.45, 99.75, 55.59, 54.63, 48.77, 45.74, 45.65, 37.28, 18.74. HRMS (ESI): exact mass calcd for $C_{30}H_{36}N_8O_3$ [M + H]$^+$, 557.2983, found 557.2985.

*N-(3-(3-Cyclopropyl-7-(2-methoxy-4-(4-methylpiperazin-1-yl)-phenylamino)-2-oxo-3,4-dihydropyrimido[4,5-d]pyrimidin-1(2H)-yl)phenyl)acrylamide (**2p**).* ^{1}H NMR (400 MHz, DMSO-d_6) δ 10.31 (s, 1H), 8.12 (s, 1H), 7.81 (d, J = 7.6 Hz, 1H), 7.55 (s, 1H), 7.48 (s, 1H), 7.43 (t, J = 8.0 Hz, 1H), 7.27 (d, J = 7.6 Hz, 1H), 6.96 (d, J = 7.6 Hz, 1H), 6.50 (s, 1H), 6.43 (dd, J = 10.0, 17.2 Hz, 1H), 6.25 (d, J = 16.8 Hz, 1H), 6.03 (s, 1H), 5.76 (d, J = 10.0 Hz, 1H), 4.43 (s, 2H), 3.75 (s, 3H), 3.00 (m, 4H), 2.67 (m, 1H), 2.46 (m, 4H), 2.24 (s, 3H), 0.76 (d, J = 5.6 Hz, 2H), 0.68 (m, 2H). ^{13}C NMR (125 MHz, DMSO-d_6) δ 163.11, 158.27, 157.11, 154.01, 153.89, 146.78, 139.49, 137.42, 131.74, 128.91, 126.92, 124.91, 120.77, 120.73, 118.28, 106.41, 101.87, 99.74, 55.59, 54.62, 48.76, 45.74, 44.50, 30.04, 6.86. HRMS (ESI): exact mass calcd for $C_{30}H_{34}N_8O_3$ [M + H]$^+$, 555.2827, found 555.2821.

*N-(3-(7-(2-Methoxy-4-(4-methylpiperazin-1-yl)phenylamino)-2-oxo-3-phenyl-3,4-dihydropyrimido[4,5-d]pyrimidin-1(2H)-yl)-phenyl)acrylamide (**2q**).* ^{1}H NMR (400 MHz, DMSO-d_6) δ 10.32 (s, 1H), 8.17 (s, 1H), 7.82 (d, J = 8.0 Hz, 1H), 7.68 (s, 1H), 7.56 (s, 1H), 7.41−7.47 (m, 5H), 7.26−7.32 (m, 2H), 7.07 (d, J = 7.6 Hz, 1H), 6.52 (d, J = 2.0 Hz, 1H), 6.44 (dd, J = 10.0, 16.8 Hz, 1H), 6.26 (dd, J = 1.6, 16.8 Hz, 1H), 6.05 (d, J = 7.2 Hz, 1H), 5.76 (d, J = 11.6 Hz, 1H), 4.87 (s, 2H), 3.77 (s, 3H), 3.01 (m, 4H), 2.43 (m, 4H), 2.22 (s, 3H). ^{13}C NMR (125 MHz, DMSO-d_6) δ 163.14, 158.43, 157.20, 154.08, 152.17, 146.90, 142.39, 139.53, 137.28, 131.75, 128.97, 128.73, 126.96, 126.16, 125.60, 124.98, 120.79, 120.70, 118.44, 106.42, 101.82, 99.76, 55.61, 54.63, 48.75, 46.74, 45.75. HRMS (ESI): exact mass calcd for $C_{33}H_{34}N_8O_3$ [M + H]$^+$, 591.2827, found 591.2823.

*N-(3-(7-(2-Methoxy-4-(4-methylpiperazin-1-yl)phenylamino)-3-(naphthalen-1-yl)-2-oxo-3,4-dihydropyrimido[4,5-d]pyrimidin-1(2H)-yl)phenyl)acrylamide (**2r**).* ^{1}H NMR (400 MHz, DMSO-d_6) δ 10.34 (s, 1H), 8.21 (s, 1H), 7.93−7.97 (m, 4H), 7.83 (d, J = 8.4 Hz, 1H), 7.72 (s, 1H), 7.63 (dd, J = 2.0, 8.4 Hz, 1H), 7.59 (s, 1H), 7.50−7.57 (m, 2H), 7.47 (t, J = 8.0 Hz, 1H), 7.33 (d, J = 8.8 Hz, 1H), 7.11 (d, J = 7.6 Hz, 1H), 6.53 (d, J = 2.0 Hz, 1H), 6.45 (dd, J = 10.0, 16.8 Hz, 1H), 6.26 (dd, J = 1.6, 16.8 Hz, 1H), 6.06 (d, J = 8.0 Hz, 1H), 5.77 (dd, J = 1.6, 10.0 Hz, 1H), 5.01 (s, 2H), 3.78 (s, 3H), 3.01 (m, 4H), 2.44 (m, 4H), 2.22 (s, 3H). ^{13}C NMR (125 MHz, DMSO-d_6) δ 163.15, 158.48, 157.18, 154.11, 152.35, 140.09, 139.54, 137.25, 133.06, 131.75, 131.09, 128.98, 127.95, 127.52, 127.46, 126.94, 126.38, 125.89, 124.99, 122.26, 120.81, 120.71, 118.49, 106.44, 101.91, 99.78, 55.62, 54.57, 48.68, 46.74, 45.65. HRMS (ESI): exact mass calcd for $C_{37}H_{36}N_8O_3$ [M + H]$^+$, 641.2983, found 641.2985.

*N-(3-(3-Benzyl-7-(2-methoxy-4-(4-methylpiperazin-1-yl)-phenylamino)-2-oxo-3,4-dihydropyrimido[4,5-d]pyrimidin-1(2H)-yl)phenyl)acrylamide (**2s**).* ^{1}H NMR (400 MHz, DMSO-d_6) δ 10.30 (s, 1H), 8.08 (s, 1H), 7.84 (d, J = 8.0 Hz, 1H), 7.60 (s, 1H), 7.49 (s, 1H), 7.45 (t, J = 8.0 Hz, 1H), 7.33−7.41 (m, 4H), 7.26−7.32 (m, 1H), 7.02 (d, J = 7.6 Hz, 1H), 6.50 (d, J = 2.4 Hz, 1H), 6.43 (dd, J = 10.0, 16.4 Hz, 1H), 6.25 (dd, J = 2.0, 16.8 Hz, 1H), 6.03 (d, J = 6.8 Hz, 1H), 5.76 (dd, J = 2.0, 10.0 Hz, 1H), 4.64 (s, 2H), 4.40 (s, 2H), 3.75 (s, 3H), 2.99 (t, J = 4.8 Hz, 4H), 2.42 (t, J = 4.8 Hz, 4H), 2.21 (s, 3H). ^{13}C NMR (125 MHz, DMSO-d_6) δ 163.14, 158.28, 157.08, 154.24, 152.61, 146.81, 139.51, 137.49, 136.68, 131.75, 128.96, 128.61, 127.75, 127.40, 126.94, 125.00, 120.77, 120.73, 118.35, 106.41, 101.00, 99.74, 55.61, 54.63, 50.52, 48.75, 45.75, 43.73. HRMS (ESI): exact mass calcd for $C_{34}H_{36}N_8O_3$ [M + H]$^+$, 605.2983, found 605.2984.

*N-(3-(3-(Biphenyl-4-yl)-7-(2-methoxy-4-(4-methylpiperazin-1-yl)-phenylamino)-2-oxo-3,4-dihydropyrimido[4,5-d]pyrimidin-1(2H)-yl)phenyl)acrylamide (**2t**).* ^{1}H NMR (400 MHz, DMSO-d_6) δ 10.33 (s, 1H), 8.19 (s, 1H), 7.83 (d, J = 7.6 Hz, 1H), 7.69−7.74 (m, 5H), 7.46−7.58 (m, 6H), 7.37 (t, J = 7.2 Hz, 1H), 7.32 (d, J = 8.8 Hz, 1H), 7.09 (d, J = 7.6 Hz, 1H), 6.52 (s, 1H), 6.45 (dd, J = 10.0, 16.4 Hz, 1H), 6.26 (d, J = 16.8 Hz, 1H), 6.06 (d, J = 6.8 Hz, 1H), 5.77 (d, J = 10.0 Hz, 1H), 4.92 (s, 2H), 3.77 (s, 3H), 3.01 (m, 4H), 2.43 (m, 4H), 2.22 (s, 3H). ^{13}C NMR (125 MHz, DMSO-d_6) δ 163.14, 158.44, 157.17, 154.09, 152.15, 146.93, 141.69, 139.54, 139.43, 137.78, 137.27, 131.74, 128.97, 128.91, 127.41, 126.94, 126.88, 126.58, 125.83, 124.98, 120.80, 120.71, 118.46, 106.43, 101.81, 99.76, 55.61, 54.60, 48.71, 46.60, 45.70. HRMS (ESI): exact mass calcd for $C_{39}H_{38}N_8O_3$ [M + H]$^+$, 667.3140, found 667.3146.

*N-(3-(7-(2-Methoxy-4-(4-methylpiperazin-1-yl)phenylamino)-2-oxo-3-(4-phenoxyphenyl)-3,4-dihydropyrimido[4,5-d]pyrimidin-1(2H)-yl)phenyl)acrylamide (**2u**).* ^{1}H NMR (400 MHz, DMSO-d_6) δ 10.32 (s, 1H), 8.17 (s, 1H), 7.81 (d, J = 8.4 Hz, 1H), 7.67 (s, 1H), 7.56 (s, 1H), 7.40−7.47 (m, 5H), 7.30 (d, J = 8.8 Hz, 1H), 7.16 (t, J = 7.6 Hz, 1H), 7.04−7.07 (m, 5H), 6.52 (d, J = 2.4 Hz, 1H), 6.44 (dd, J = 10.0, 16.8 Hz, 1H), 6.25 (dd, J = 2.0, 16.8 Hz, 1H), 6.04 (s, 1H), 5.76 (dd, J = 2.0, 10.0 Hz, 1H), 4.86 (s, 2H), 3.77 (s, 3H), 3.00 (t, J = 4.4 Hz, 4H), 2.43 (t, J = 4.4 Hz, 4H), 2.22 (s, 3H). ^{13}C NMR (125 MHz, DMSO-d_6) δ 163.13, 158.40, 157.19, 156.49, 154.71, 154.07, 152.20, 146.90, 139.51, 137.69, 137.27, 131.74, 130.07, 128.95, 127.46, 126.94, 124.96, 123.61, 120.77, 120.70, 118.73, 118.61, 118.41, 106.41, 101.77, 99.75, 55.61, 54.62, 48.73, 47.01, 45.73. HRMS (ESI): exact mass calcd for $C_{39}H_{38}N_8O_4$ [M + H]$^+$, 683.3089, found 683.3095.

*N-(3-(3-(4-(Benzyloxy)phenyl)-7-(2-methoxy-4-(4-methylpiperazin-1-yl)phenylamino)-2-oxo-3,4-dihydropyrimido[4,5-d]pyrimidin-1(2H)-yl)phenyl)acrylamide (**2v**).* ^{1}H NMR (400 MHz, DMSO-d_6) δ 10.31 (s, 1H), 8.15 (s, 1H), 7.81 (d, J = 8.4 Hz, 1H), 7.66 (s, 1H), 7.54 (s, 1H), 7.29−7.47 (m, 8H), 7.04−7.07 (m, 3H), 6.52 (d, J = 2.0 Hz, 1H), 6.44 (dd, J = 10.0, 16.8 Hz, 1H), 6.25 (dd, J = 2.0, 16.8 Hz, 1H), 6.05 (d, J = 8.0 Hz, 1H), 5.76 (dd, J = 2.0, 10.0 Hz, 1H), 5.13 (s, 2H), 4.81 (s, 2H), 3.77 (s, 3H), 3.00 (t, J = 4.4 Hz, 4H), 2.42 (t, J = 4.4 Hz, 4H), 2.22(s, 3H). ^{13}C NMR (125 MHz, DMSO-d_6) δ 163.13, 158.37, 157.23, 156.52, 154.03, 152.21, 146.84, 139.51, 137.33, 136.97, 135.44, 131.74, 128.93, 128.39, 127.79, 127.63, 127.13, 126.93, 124.97, 120.78, 120.72, 118.37, 114.89, 106.42, 101.77, 99.75, 69.36, 55.61, 54.63, 48.75, 47.24, 45.75. HRMS (ESI): exact mass calcd for $C_{40}H_{40}N_8O_4$ [M + H]$^+$, 697.3245, found 697.3252.

*N-(3-(7-(2-Methoxy-4-(4-methylpiperazin-1-yl)phenylamino)-3-methyl-2-oxo-3,4-dihydropyrimido[4,5-d]pyrimidin-1(2H)-yl)-phenyl)propionamide (**2x**).* ^{1}H NMR (400 MHz, DMSO-d_6) δ 9.99 (s, 1H), 8.10 (s, 1H), 7.69 (d, J = 8.4 Hz, 1H), 7.50 (s, 1H), 7.46 (s, 1H), 7.39 (t, J = 8.0 Hz, 1H), 7.26 (d, J = 8.4 Hz, 1H), 6.90 (d, J = 8.0 Hz, 1H), 6.51 (d, J = 2.4 Hz, 1H), 6.03 (d, J = 7.6 Hz, 1H), 4.45 (s, 2H), 3.76 (s, 3H), 3.01 (t, J = 4.4 Hz, 4H), 2.96 (s, 3H), 2.43 (t, J = 4.4 Hz, 4H), 2.30 (q, J = 7.2, 14.8 Hz, 2H), 2.22 (s, 3H), 1.06 (t, J = 7.2 Hz, 3H). ^{13}C NMR (125 MHz, DMSO-d_6) δ171.97, 158.24, 157.26, 153.99, 152.54, 146.78, 139.89, 137.41, 128.76, 124.32, 120.79, 120.31, 117.87, 106.44, 101.13, 99.74, 55.61, 54.66, 48.79, 45.81, 45.75, 39.00, 29.55, 9.60. HRMS (ESI): exact mass calcd for $C_{28}H_{34}N_8O_3$ [M + H]$^+$, 531.2827, found 531.2819.

Cell Lines and Reagents. H1975 (NSCLC, EGFR$^{L858R/T790M}$), HCC827 (NSCLC, EGFR $^{del\ E746\text{-}A750}$), A431 (epidermoid carcinoma, EGFR overexpression), and A549 (NSCLC, EGFR wild type) cells were obtained from ATCC. The cells were maintained at 37 °C in a 5% CO_2 incubator in RPMI 1640 (Gibco, Invitrogen) containing 10% fetal bovine serum (Gibco, Invitrogen). HLF-1(diploid human lung fibroblasts) and HL-7702 (diploid human liver cell) were gifts from Prof. Duanqing Pei. The HLF-1 was maintained in Ham's F12K medium (Gibco, Invitrogen) with 15% FBS. The HL-7702 was

cultured in RPMI 1640 containing 10% FBS. The EGFR gene of every cell line was sequenced before use. Gefitinib was synthesized in our chemistry laboratory.

In Vitro Enzymatic Activity Assay. Wild type and different EGFR mutants (T790M, L858R, L861Q, L858R/T790M) and the Z′-Lyte Kinase Assay Kit were purchased from Invitrogen. Ten concentration gradients from 5.1×10^{-11} to 1.0×10^{-6} mol/L were set for all the tested compounds. The experiments were performed according to the instructions of the manufacturer.

Kinase Profiling Study and K_d Determination. The kinase profiling study and K_d determination were conducted using the Ambit Kinome screening platform (www.kinomescan.com). Kinases were produced displayed on T7 phage or by expression in HEK-293 cells and tagged with DNA. Binding reactions were performed at r.t. for 1 h, and the fraction of kinase not bound to test compound was determined by capture with an immobilized affinity ligand and quantitation by quantitative PCR. Each kinase was tested individually against each compound. K_d values were determined using 11 serial 3-fold dilutions and presented as mean values from experiments performed in duplicate.

Cell Proliferation and Growth Inhibition Assay. Cell proliferation was assessed by MTS assay. The cells were exposed to treatment for 72 h, and the number of cells used per experiment for each cell line was adjusted to obtain an absorbance of 1.3 to 2.2 at 490 nm. Six concentrations (0.1 nM to 10 μM) were set for the compounds. At least six parallels of every concentration were used. All experiments were repeated at least four times. The data were calculated using GraphPad Prism version 4.0. The IC_{50} were fitted using a nonlinear regression model with a sigmoidal dose−response.

Colony Formation Assay. The H1975 cells were plated in 6-cm dishes with densities of 500 cells/dish. After 24-h growth, the cells were treated with compounds **2q** and **2s** under concentrations ranging from 0.1 to 10 nM. The medium with compounds were changed every 3 days. After 9-day incubation, plates were fixed with 4% formaldehyde, and 0.2% crystal violet was used for staining.

Antibodies and Western Blotting. Cells were plated in 6-cm dishes. After 24-h growth, the cells were treated with the compounds under the indicated concentrations for 24 h. Cell lysates were collected with 1× lysis buffer (CST) and were briefly sonicated. Western blot analyses were conducted after separation by SDS/PAGE electrophoresis and transfer to PVDF membranes. Membranes were blocked in 5% bovine serum albumin/TBST and probed with the indicated antibodies, followed by a peroxidase-conjugated antimouse or rabbit secondary antibody. Blots were developed by enhanced chemiluminescence (Thermo). Anti-phospho Akt (Ser 173), anti-total Akt, anti-EGFR, anti-phospho specific EGFR (pY1068), anti-total ERK1/2, and anti-phospho ERK1/2 (pT202/pY204) antibodies were obtained from Cell Signaling Technology.

Flow Cytometry Assay. For the apoptosis assay, cells were plated in six-well plates overnight and were treated with the compounds under indicated concentrations for 48 h. Trypsin (0.25%) was used, and a single cell suspension was prepared according to the instructions of the manufacturer. Apoptosis was assessed using a PE-Annexin V Kit (BD Pharmingen). The samples were detected with a FACS Calibur flow cytometer (Becton Dickinson)

The cell cycle analysis was performed by using Cycletest Plus DNA Reagent Kit (BD Pharmingen). Cells seeded in six-well plates were serum-starved for 24 h to synchronize cells in the G0−G1 phase of the cell cycle. Then the cells were treated with **2q** and **2s** under the indicated concentrations for 24 h. The cells were lightly trypsinized, and samples were prepared according to the instructions of the manufacturer. Samples were analyzed on a FACS Calibur flow cytometer (Becton Dickinson), and data were analyzed using the Modfit software package.

Mouse Tumor Xenograft Efficacy Study. The efficacy study was conducted in accordance with the guidelines for the Care and Use of Laboratory Animals in Guangzhou Institute of Biomedicine and Health (GIBH, CAS). Six week old SCID mice were inoculated subcutaneously with H1975 NSCLC cells (2×10^6/mouse) in the right flank. Upon reaching an average tumor volume of 380−420 mm^3 (10−12 days post implantation), animals were randomized into treatment groups (n = 6 mice/group). Each group was dosed orally for 14 days with either vehicle only or with compound **2s** at 10 or 30 mg/kg or gefitinib at 50 mg/kg daily (qd). The doses were in a volume of 0.1 mL/20 g of the animal body weight. Tumor volumes were measured every other day using vernier calipers, and volumes were calculated using the following formula: tumor volume (mm^3) = $W^2(L/2)$, where W = width and L = length in mm.

■ ASSOCIATED CONTENT

Ⓢ Supporting Information

^{1}H NMR spectrum and purity determination for compounds **2a−x**, apoptosis, cell cycle arrest, and colony formation inhibition induced by compounds **2q** and **2s**, Western blot analysis on A549 and A431 cells, growth inhibition on HLF-1 cells. This material is available free of charge via the Internet at http://pubs.acs.org.

■ AUTHOR INFORMATION

Corresponding Author

*Tel: +86-20-32015276. Fax: +86-20-32015299. E-mail: ding_ke@gibh.ac.cn.

Author Contributions

#These authors contributed equally to this work.

Notes

The authors declare no competing financial interest.

■ ACKNOWLEDGMENTS

We thank National Basic Research Program of China (# 2010CB529706, 2009CB940904), National Natural Science Foundation (# 21072192), Key Project on Innovative Drug of Guangdong Province (# 2011A080501013), Strategic Collaborative Project of Guangdong Province and Chinese Academy of Sciences, Key Project on Innovative Drug of Guangzhou City (grant # 2009Z1-E911, 2010J-E551), and the 100-talent program of Chinese Academy of Sciences (CAS) for their financial support.

■ ABBREVIATIONS USED

T, threonine; M, methionine; I, isoleucine; L, leucine; R, arginine; E, glutamic acid; A, alanine; Q, glutamine; EGFR, epidermal growth factor receptor; WT, wild-type; NSCLC, non small cell lung cancer; ATP, adenosine-triphosphate; LAH, lithium aluminum hydride; *m*-CPBA, 3-chloroperbenzoic acid; DIPEA, *N*,*N*-diisopropylethylamine; JAK3, Janus kinase 3; K_d, binding constant; BLK, B lymphocyte kinase; BTK, Bruton's tyrosine kinase; GAK, cyclin G associated kinase; FRK, Fyn-related kinase; LCK, lymphocyte-specific protein tyrosine kinase; MAPK, mitogen-activated protein kinase signaling pathway

■ REFERENCES

(1) Olayioye, M. A.; Neve, R. M.; Lane, H. A.; Hynes, N. E. The ErbB signaling network: receptor heterodimerization in development and cancer. *EMBO J.* **2000**, *19*, 3159−3167.

(2) Ciaardiello., F.; Tortora, G. EGFR antagonists in cancer treatment. *N. Engl. J. Med.* **2008**, *358*, 1160−1174.

(3) Yun, C. H.; Boggon, T. J.; Li, Y.; Woo, M. S.; Greulich, H.; Meyerson, M.; Eck, M. J. Structures of lung cancer-derived EGFR mutants and inhibitor complexes: mechanism of activation and insights into differential inhibitor sensitivity. *Cancer Cell* **2007**, *11*, 217−227.

(4) Carey, K. D.; Garton, A. J.; Romero, M. S.; Kahler, J.; Thomson, S.; Ross, S.; Park, F.; Haley, J. D.; Gibson, N.; Sliwkowski, M. X. Kinetic analysis of epidermal growth factor receptor somatic mutant

proteins shows increased sensitivity to the epidermal growth factor receptor tyrosine kinase inhibitor, erlotinib. *Cancer Res.* **2006**, *66*, 8163−8171.

(5) (a) Bokemeyer, C.; Bondarenko, I.; Makhson, A.; Hartmann, J. T.; Aparicio, J.; de Braud, F.; Donea, S.; Ludwig, H.; Schuch, G.; Stroh, C.; Loos, A. H.; Zubel, A.; Koralewski, P. Fluorouracil, leucovorin, and oxaliplatin with and without cetuximab in the first-line treatment of metastatic colorectal cancer. *J. Clin. Oncol.* **2009**, *27*, 663−671. (b) Van Cutsem, E.; Köhne, C. H.; Hitre, E.; Zaluski, J.; Chang, C. C. R.; Makhson, A.; D'Haens, G.; Pintér, T.; Lim, R.; Bodoky, G.; Roh, J. K.; Folprecht, G.; Ruff, P.; Stroh, C.; Tejpar, S.; Schlichting, M.; Nippgen, J.; Rougier, P. Cetuximab and chemotherapy as initial treatment for metastatic colorectal cancer. *N. Engl. J. Med.* **2009**, *360*, 1408−1417.

(6) Giusti, R. M.; Shastri, K. A.; Cohen, M. H.; Keegan, P.; Pazdur, R. FDA drug approval summary: panitumumab (Vectibix). *Oncologist* **2007**, *12*, 577−583.

(7) (a) Pallis, A.; Briasoulis, E.; Linardou, H.; Papadimitriiou, C.; Bafaloukos, D.; Kosmidis, P.; Murray, S. Mechanisms of resistance to epidermal growth factor receptor tyrosine kinase inhibitors in patients with advanced non-small-cell lung cancer: clinical and molecular considerations. *Curr. Med. Chem.* **2011**, *18*, 1613−1628. (b) Oxnard, G. R.; Arcila, M. E.; Chemieleck, J.; Ladany, M.; Miller, V. A.; Pao, W. New strategies in overcoming acquired resistance to epidermal growth factor receptor tyrosine kinase inhibitors in lung cancer. *Clin. Cancer Res.* **2011**, *17*, 5530−5537.

(8) (a) Pao, W; Miller, V. A.; Politi1, K. A.; Riely, G. J.; Somwar, R.; Zakowski, M. F.; Kris, M. G.; Varmus, H. Acquired resistance of lung adenocarcinomas to gefitinib or erlotinib is associated with a second mutation in the EGFR kinase domain. *PLoS Med.* **2005**, *2*, 1−11. (b) Kobayashi, S.; Boggon, T. J.; Dayaram, T.; Jänne, P. A.; Kocher, O.; Meyerson, M.; Johnson, B. E.; Eck, M. J.; Tenen, D. G.; Halmos, B. EGFR mutation and resistance of non-small-cell lung cancer to gefitinib. *N. Engl. J. Med.* **2005**, *352*, 786−792.

(9) Lu, X.; Cai, Q.; Ke Ding, K. Recent developments in the third generation inhibitors of Bcr-Abl for overriding T315I mutation. *Curr. Med. Chem.* **2011**, *18*, 2146−2157.

(10) Yun, C.-H.; Mengwasser, K. E.; Toms, A. V.; Woo, M. S.; Greulich, H.; Wong, K.-K.; Meyerson, M.; Eck, M. J. The T790M mutation in EGFR kinase causes drug resistance by increasing the affinity for ATP. *Proc. Natl. Acad. Sci. U.S.A.* **2008**, *105*, 2070−2075.

(11) Recent examples see: (a) Wu, C.-H.; Coumar, M. S.; Chu, C.-Y.; Lin, W.-H.; Chen, Y.-R.; Chen, C.-T.; Shiao, H.-Y.; Rafi, S.; Wang, S.-Y.; Hsu, H.; Chen, C.-H.; Chang, C.-Y.; Chang, T.-Y.; Lien, T.-W.; Fang, M.-Y.; Chen, C.-P.; Yeh, T.-K.; Hsu, J. T.-A; Liao, C.-C.; Chao, Y.-S.; Hsieh, H.-P. Design and synthesis of tetrahydropyridothieno-[2,3-*d*]pyrimidine scaffold based epidermal growth factor receptor (EGFR) kinase inhibitors: The role of side chain chirality and Michael acceptor group for maximal potency. *J. Med. Chem.* **2010**, *53*, 7316−7326. (b) Carmi, C.; Cavazzoni, A.; Vezzosi, S.; Bordi, F.; Vacondio, F.; Silva, C.; Rivara, S.; Lodola, A.; Alfieri, R. R.; Monica, S. L.; Galetti, M.; Ardizzoni, A.; Petronini, P. G.; Mor, M. Novel irreversible epidermal growth factor receptor inhibitors by chemical modulation of the cysteine-trap portion. *J. Med. Chem.* **2010**, *53*, 2038−2050. (c) Bikker, J. A.; Brooijmans, N.; Wissner, A.; Mansour, T. S. Kinase domain mutations in cancer: implications for small molecule drug design strategies. *J. Med. Chem.* **2009**, *52*, 1493−1509. (d) Cha, M. Y.; Lee, K.-O.; Kim, J. W.; Lee, C. G.; Song, J. Y.; Kim, Y. H.; Lee, G. S.; Park, S. B.; Kim, M. S. Discovery of A novel Her-1/Her-2 dual tyrosine kinase inhibitor for the treatment of Her-1 selective inhibitor-resistant non-small cell lung cancer. *J. Med. Chem.* **2009**, *52*, 6880−6888. (e) Coumar, M. S.; Chu, C.-Y.; Lin, C.-W.; Shiao, H.-Y.; Ho, Y.-L.; Reddy, R.; Lin, W.-H.; Chen, C.-H.; Peng, Y.-H.; Leou, J.-S.; Lien, T.-W.; Huang, C.-T.; Fang, M.-Y.; Wu, S.-H.; Wu, J.-S.; Chittimalla, S.-K.; Song, J.-S.; Hsu, J.-T. A.; Wu, S.-Y.; Liao, C.-C.; Chao, Y.-S.; Hsieh, H.-P. Fast-forwarding hit to lead: Aurora and epidermal growth factor receptor kinase inhibitor lead identification. *J. Med. Chem.* **2010**, *53*, 4980−4988.

(12) (a) Smaill, J. B.; Showalter, H. D. H.; Zhou, H.; Bridges, A. J.; McNamara, D. J.; Fry, D. W.; Nelson, J. M.; Sherwood, V.; Vincent, P. W.; Roberts, B. J.; Elliott, W. L.; Denny, W. A. Tyrosine kinase inhibitors. 18. 6-Substituted 4-anilinoquinazolines and 4-anilinopyrido-[3,4-*d*]pyrimidines as soluble, irreversible inhibitors of the epidermal growth factor receptor. *J. Med. Chem.* **2001**, *44*, 429−440. (b) Smaill, J. B.; Rewcastle, G. W.; Loo, J. A.; Greis, K. D.; Chan, O. H.; Reyner, E. L.; Lipka, E.; Showalter, H. D. H.; Vincent, P. W.; Elliott, W. L.; Denny, W. A. Tyrosine kinase inhibitors: 17. Irreversible inhibitors of the epidermal growth factor receptor: 4-(phenylamino)quinazoline- and 4-(phenylamino)pyrido[3,2-*d*]pyrimidine-6-acrylamides bearing additional solubilizing functions. *J. Med. Chem.* **2000**, *43*, 1380−1397.

(13) Li, D.; Ambrogio, L.; Shimamura, T.; Kubo, S.; Takahashi, M.; Chirieac, L. R.; Padera, R. F.; Shapiro, G. I.; Baum, A.; Himmelsbach, F.; Rettig, W. J.; Meyerson, M.; Solca, F.; Greulich, H.; Wong, K. K. BIBW2992, an irreversible EGFR/HER2 inhibitor highly effective in preclinical lung cancer models. *Oncogene* **2008**, *27*, 4702−4711.

(14) (a) Tsou, H. R.; Overbeek-Klumpers, E. G.; Hallett, W. A.; Reich, M. F.; Floyd, M. B.; Johnson, B. D.; Michalak, R. S.; Shen, R.; Shi, X.; Wang, Y. F.; Upeslacis, J.; Wissner, A. Optimization of 6,7-disubstituted-4-(arylamino)quinoline-3-carbonitriles as orally active, irreversible inhibitors of human epidermal growth factor receptor-2 kinase activity. *J. Med. Chem.* **2005**, *48*, 1107−1131. (b) Wissner, A.; Overbeek, E.; Reich, M. F.; Floyd, M. B.; Johnson, B. D.; Mamuya, N.; Rosfjord, E. C.; Discafani, C.; Davis, R.; Shi, X.; Rabindran, S. K.; Gruber, B. C.; Ye, F.; Hallett, W. A.; Nilakantan, R.; Shen, R.; Wang, Y.; Greenberger, L. M.; Tsou, H. Synthesis and structure−activity relationships of 6,7-disubstituted 4-anilinoquinoline-3-carbonitriles: The design of an orally active, irreversible inhibitor of the tyrosine kinase activity of the epidermal growth factor receptor (EGFR) and the human epidermal growth factor receptor-2 (HER-2). *J. Med. Chem.* **2003**, *46*, 49−63.

(15) Engelman, J. A.; Zejnullahu, F.; Gale, C.-M.; Lifshits, E.; Gonzales, A. J.; Shimamura, T.; Zhao, F.; Vincent, P. W.; Naumov, G. N.; Bradner, J. E.; Althaus, I. W.; Gandhi, L.; Shapiro, G. I.; Nelson, J. M.; Heymach, J. V.; Meyerson, M.; Wong, K.-K.; Jänne, P. A. PF00299804, an irreversible Pan-ERBB inhibitor, is effective in lung cancer models with EGFR and ERBB2 mutations that are resistant to gefitinib. *Cancer Res.* **2007**, *67*, 11924−31192.

(16) (a) Leproult, E.; Barluenga, S.; Moras, D.; Wurtz, J.-M.; Winssinger, N. Cysteine mapping in conformationally distinct kinase nucleotide binding sites: Application to the design of selective covalent inhibitors. *J. Med. Chem.* **2011**, *54*, 1347−1355. (b) Potashman, M. H.; Duggan, M. E. Covalent modifiers: An orthogonal approach to drug design. *J. Med. Chem.* **2009**, *52*, 1231−1246.

(17) Sequist, L. V.; Besse, B.; Lynch, T. J.; Miller, V. A.; Wong, K. K.; Gitlitz, B.; Eaton, K.; Zacharchuk, C.; Freyman, A.; Powell, C.; Ananthakrishnan, R.; Quinn, S.; Soria, J. C. Neratinib, an irreversible pan-ErbB receptor tyrosine kinase inhibitor: Results of a phase II trial in patients with advanced non-small-cell lung cancer. *J. Clin. Oncol.* **2010**, *28*, 3076−3083.

(18) Campbell, A.; Reckamp, K. L.; Camidge, D. R.; Giaccone, G.; Gadgeel, S. M.; Khuri, F. R.; Engelman, J. A.; Denis, L. J.; O'Connell, J. P.; Janne, P. A. PF-00299804 (PF299) patient (pt)-reported outcomes (PROs) and efficacy in adenocarcinoma (adeno) and nonadeno non-small cell lung cancer (NSCLC): A phase (P) II trial in advanced NSCLC after failure of chemotherapy (CT) and erlotinib (E). *J. Clin. Oncol.* **2010**, *28*, 7596 (suppl; abstr).

(19) Yang, C.; Hirsh, V.; Cadranel, J.; Chen, Y.; Park, K.; Kim, S.; Chao, T.; Oberdick, M.; Shahidi, M; Miller, V. Phase IIb/III double-blind randomized trial of BIBW 2992, an irreversible, dual inhibitor of EGFR and HER2 plus best supportive care (BSC) versus placebo plus BSC in patients with NSCLC failing 1−2 lines of chemotherapy (CT) and erlotinib or gefitinib (LUX- Lung1). *Ann. Oncol.* **2010**, *21*, LBA1.

(20) Janjigian, Y. Y.; Groen, H. J.; Horn, L.; Smit, E. F.; Fu, Y.; Wang, F.; Shahidi, M.; Denis, L. J.; Pao, W.; Miller, V. A. Activity and tolerability of afatinib (BIBW 2992) and cetuximab in NSCLC patients with acquired resistance to erlotinib or gefitinib. *J. Clin. Oncol.* **2011**, *29*, 7525 (suppl; abstr).

(21) (a) Zhou, W.; Ercan, D.; Chen, L.; Yuan, C.-H.; Li, D.; Capelletti, M.; Cortot, A. B.; Chirieac, L.; Lacob, R. E.; Padera, R.;

Engen, J. R.; Wong, K.-K.; Eck, M. J.; Gray, N. S.; Janne, P. A. Novel mutant-selective EGFR kinase inhibitors against EGFR T790M. *Nature* **2009**, *462*, 1070−1074. (b) Zhou, W.; Ercan, D.; Janne, P. A.; Gray, N. Discovery of selective irreversible inhibitors for EGFR-T790M. *Bioorg. Med. Chem. Lett.* **2011**, *21*, 638−643.

(22) (a) Jare-Erijma, E. A.; Jov, T. M. FRET imaging. *Nat. Biotechnol.* **2003**, *21*, 1387−1395. (b) The assay was performed based on the manufacturer's instructions (Invitrogen).

(23) Steiner, P.; Joynes, C.; Bassi, R.; Wang, S.; Tonra, J. R.; Hadari, Y. R.; Hicklin, D. J. Tumor growth inhibition with cetuximab and chemotherapy in non-small cell lung cancer xenografts expressing wild-type and mutated epidermal growth factor receptor. *Clin. Cancer Res.* **2007**, *13*, 1540−1551.

(24) Libermann, T. A.; Nusbaum, H. R.; Razon, N.; Kris, R.; Lax, I.; Soreq, H.; Whittle, N.; Waterfield, M. D.; Ullrich, A.; Schlessinger, J. Amplification, enhanced expression and possible rearrangement of egf receptor gene in primary human-brain tumors of glial origin. *Nature* **1985**, *313*, 144−147.

(25) Mukohara, T.; Engelman, J. A.; Hanna, N. H.; Yeap, B. Y.; Kobayashi, S.; Lindeman, N.; Halmos, B.; Pearlberg, J.; Tsuchihashi, Z.; Cantley, L. C.; Tenen, D. G.; Johnson, B. E.; Janne, P. A. Differential effects of gefitinib and cetuximab on non-small-cell lung cancers bearing epidermal growth factor receptor mutations. *J. Natl. Cancer Inst.* **2005**, *97*, 1185−1194.

(26) Wei, Y. M.; Cao, X. Z.; Ou, Y. X.; Lu, J. H.; Xing, C. P.; Zheng, R. L. SeO2 induces apoptosis with down-regulation of Bcl-2 and up-regulation of P53 expression in both immortal human hepatic cell line and hepatoma cell line. *Mutat. Res.: Genet. Toxicol. Environ. Mutagen* **2001**, *490*, 113−121.

(27) Breul, K. H. B. S. D.; Hance, A. J.; Schafer, M. P R; Berg, A; Crystal, R G. Control of collagen production by human diploid lung fibroblasts. *J. Biol. Chem.* **1980**, *255*, 5250−5260.

(28) Toulany, M.; Dittmann, K.; Kruger, M.; Baumann, M.; Rodemann, H. P. Radioresistance of K-Ras mutated human tumor cells is mediated through EGFR-dependent activation of PI3K-AKT pathway. *Radiother. Oncol.* **2005**, *76*, 143−150.

(29) Choi, H. G.; Ren, P.; Adrian, F; Sun., F; Lee, H. S.; Wang, X.; Ding, Q.; Zhang, G.; Xie, Y.; Zhang, J.; Liu, Y.; Tuntland, T.; Warmuth, M.; Manley, P. W.; Mestan, J.; Gray, N. S.; Sim, T. A type-II kinase inhibitor capable of inhibiting the T315I "gatekeeper" mutant of Bcr-Abl. *J. Med. Chem.* **2010**, *53*, 5439−5448.

(30) Paulsen, C. E.; Truong, T. H.; Garcia, F. J.; Homann, A.; Gupta, V.; Leonard, S, E.; Carroll, K. S. Peroxide-dependent sulfenylation of the EGFR catalytic site enhances kinase activity. *Nat. Chem. Biol.* **2012**, *8*, 57−64.

(31) Carey, K. D.; Garton, A. J.; Romero, M. S.; Kahler, J.; Thomson, S.; Ross, S.; Park, F.; Haley, J. D.; Gibson, N.; Sliwkowski, M. X. Kinetic analysis of epidermal growth factor receptor somatic mutant proteins shows increased sensitivity to the epidermal growth factor receptor tyrosine kinase inhibitor, Erlotinib. *Cancer Res.* **2006**, *66*, 8163−8171.